The Black Hole Universe (BHU)

Enrique Darkcosmos.Com Gaztanaga

The Black Hole Universe (BHU)

Enrique Gaztañaga★
Institute of Space Sciences (ICE, CSIC), 08193 Barcelona, Spain
Institut d´ Estudis Espacials de Catalunya (IEEC), 08034 Barcelona, Spain

November 3, 2021

ABSTRACT

Observations tell us that cosmic expansion is dominated by an effective cosmological constant. This means that we live inside a trapped surface, which corresponds to a Black Hole (BH) event horizon. We show that such Black Hole Universe (BHU) is a solution to classical GR, where two nested FLRW metrics are connected by a BH event horizon. Observed CMB anomalies are consistent with such BHU. Our Universe is the first BH for which we know what is inside. The same BHU solution can also be used to model stellar or galactic BH which are not singular and have regular matter and radiation expanding inside their event horizon. Observed BHs (and possibly BHs making the Dark Matter, DM) could just be BHUs. In comoving coordinates the BHU is expanding while in Schwarzschild coordinates it is asymptotically static. Such frame duality can be directly tested with current cosmological and BH observations.

Key words: Cosmology: dark energy, cosmic background radiation, cosmological parameters, early Universe, inflation

1 INTRODUCTION

The Big Bang (BB), Dark Energy (DE) or Λ, DM and BHs are puzzles we don't yet understand at any fundamental level. The corresponding GR solutions seem to involve singularities that make no physical sense. Some theorist interpret mathematical singularity theorems as evidence that no other solutions can possibly exist and that a new theory of Quantum Gravity is needed to understand these puzzles. But this is far from settle (see Dadhich 2007) and it is outside the scope of our paper. That a non singular version of such solutions exist is clear from direct observations and common sense. Here we elaborate on a well known existing example of non singular classical solution to GR: the Bubble Universes. A domain wall, or thin bubble, that connects a region of false vacuum, with de Sitter (dS) space inside, with empty space outside. These solutions are not totally appealing because they have no regular matter and require a surface term (or bubble tension $\sigma \neq 0$) to artificially glue dS and SW metrics discontinuity (e.g. see Blau et al. 1987; Mazur & Mottola 2001; Aguirre & Johnson 2005). Our BHU proposal presented here can be thought as a new type of Bubble Universe with a FLRW interior (including regular matter and radiation) and no bubble or surface term ($\sigma = 0$). The empty space outside is just a local approximation, which is usually done to describe isolated BHs. In a more realistic situation we can interpret the BH solution to exist inside another FLRW background.

The BB and inflation are the standard cosmological models we use to interpret observations such as BAO, SN, CMB and LSS. This is despite the fact that we have no idea how the BB or inflation started. For the same reason, we don't need to proof a particular formation mechanism to consider the BHU as a possible alternative to the BB and BH paradigms. In §2.1 and 4.3, we give some ideas about how a BHU could form. But our scope and focus here is not on the formation mechanism itself but just to show that new solutions exist that can help us understanding the above puzzles at a deeper fundamental level.

A Schwarzschild BH metric (BH.SW) represents a singular object of mass M. The BH event horizon $r_{SW} \equiv 2GM$ prevent us from interacting with the inside (which makes BHs good candidates for DM). Physically, a singular point does not make any sense.[1] What is the metric inside? What happens when they accrete matter or when two BHs merge? Do BHs grow and co-evolve with galaxies (e.g. Kormendy & Ho 2013)? Do observed BH form in stellar collapse or are they seeded by primordial BHs? How do primordial BH form (e.g. Kusenko 2020)? Most of these modelings assume the BH.SW solution, but can we actually answer any of these questions if we do not have a physical model for the BH interior?

Here, we look for an alternative solution to the BH.SW interior, defined as a non singular classical object of size r_{SW} which reproduces the BH.SW metric for the outside $r > r_{SW}$. A physical BH of size $r = r_{SW}$ and mass M, has a density:

$$\rho_{BH} = \frac{M}{V} = \frac{3r_{SW}^{-2}}{8\pi G} = \frac{3M^{-2}}{32\pi G^3} \,. \tag{1}$$

The BH interior can not be made out of regular matter or radiation because according to GR a perfect fluid with mass M has a minimal radius (Buchdahl 1959):

$$R > 9/8 r_{SW}. \tag{2}$$

But objects with mass and sizes matching r_{SW} have been observed. What is inside a BH then? The highest known density for a stellar object is that of a Neutron star, which has the density of an atomic nucleus, but is still a few times larger than r_{SW}. To achieve

[1] This is why it took Newton over 20 years to publish the inverse square law of gravity. He did not need to solve Quantum Gravity to address such singularity, but he had to (re) invent integration (darkcosmos.com).

★ E-mail:gaztanaga@gmail.com

such a high density for a perfect fluid, the radial pressure inside a BH needs to be negative (Brustein & Medved 2019 and references therein). Cosmologist are used to this type of fluids, which are called Quintessence, Inflation or Dark Energy (DE). So, could the inside of a BH be DE? Mazur & Mottola (2015) have argued that the same DE repulsive force that causes cosmic acceleration could also prevent the BH singular collapse.

We find a new solution to these questions, which we call the BHU metric. We will also explore the idea that our Universe corresponds to such BHU solution. As the universe expands H tends to H_Λ which corresponds to a trapped surface $r_\Lambda = 1/H_\Lambda$, just like the event horizon of a BH. Moreover, the density of our universe in that limit is $\rho = 3H_\Lambda^2/8\pi G$ which exactly corresponds to that of a BH, in Eq.1 for $r_{SW} = r_\Lambda$. In fact, the Hubble Horizon $r_H = 1/H$ also has this property. This is not just a coincidence as advocated by some scientist (Landsberg 1984; Knutsen 2009). It directly indicates that we actually live inside a very massive physical BH. It also tells us what is the metric inside a BH: our Universe is the only object whose interior we know and has the density of a BH. We will explicitly show that such BHU is a solution to classical GR.

The idea that the universe might be generated from the inside of a BH is not new and has extensive literature (see Easson & Brandenberger 2001; Oshita & Yokoyama 2018 and references therein) which mostly focused in dS metric with a dual role of the BH interior and an approximation for our universe. Many of the formation mechanisms involve some modifications or extensions of GR, often motivated by quantum gravity or string theory. This is what we try to avoid here (see also Ellis & Silk 2014). There are also some simple scalar field $\varphi(x)$ examples (e.g. Daghigh et al. 2000) which presented models within the scope of a classical GR and classical field theory with a false vacuum (FV) interior similar to our BH.fv solution here. These models have been questioned using no-go theorems, such us that by Galtsov & Lemos (2001), that state that no smooth solution to $\varphi(x)$ can interpolate between dS and SW space. But this is not an issue for our solution for three reasons. First, the external asymptotic space is really SW+dS or FLRW (a BH is a perturbation within a FLRW metric), where solutions do exist (e.g. Dymnikova 2003). Second, we do not need $\varphi(x)$ to smoothly transit between metrics: $\varphi(x)$ is trapped in a FV, which is discontinuous by nature, as shown in the Bubble Universes (e.g. see Blau et al. 1987; Mazur & Mottola 2001; Aguirre & Johnson 2005). Finally, we do not actually need a scalar field or ρ_Λ to have a BHU solution. We just need the interior of the BH to have a FLRW metric with no bubble or surface terms.

The above solutions provide support to the idea that our universe could be inside a BH, but they are too simplistic, as they don't contain any matter or radiation. Can these ideas be extended to the FLRW metric? Several authors have grasped the idea and speculated that the FLRW metric could be the interior of a BH (Pathria 1972; Good 1972; Popławski 2016; Zhang 2018). But these previous solution were incomplete (Knutsen 2009) or outside classical GR. Stuckey (1994) showed that a FLRW metric can be joined to an outside BH.SW metric. But his solution only worked for a dust filled universe. The BHU model can also include radiation and a Λ term (or a FV), which seem to be needed to explain our universe. Here we also interpret the outside BH.SW solution as perturbation in an external FLRW and explore the BH and cosmological consequences of such solution.

Our BHU solution is quite different from that of Smolin (1992), who speculated that all final (e.g. BH) singularities 'bounce' or tunnel to initial singularities of new universes. Here we propose the opposite, that such mathematical singularities are not needed to explain the physical world. As stated by Ellis (2008), the concept of physical infinity is not a scientific one if science involves testability by either observation or experiment. The BHU model can avoid the initial causal and entropy paradoxes (Dyson et al. 2002; Penrose 2006) because BHU is within a larger (previously existing) expanding background.

In §2 we present the GR field equations of a perfect fluid for homogeneous solutions: a FV and an expanding FLRW universe. We also give a brief introduction to the general case of in-homogeneous solutions with spherical symmetry in physical SW coordinates. The FLRW solution can also be expressed in these SW coordinates. This duality is a key ingredient to find our new solutions for a physical BH interior in §3. We also discuss how these solutions apply both to BHs and to our universe. We end with a summary and a discussion of observational windows to test the BHU.

2 SOME SIMPLE SOLUTIONS

Given the Einstein-Hilbert action (Hilbert 1915; Weinberg 1972, 2008; Padmanabhan 2010):

$$S = \int_M dM \left[\frac{R - 2\Lambda}{16\pi G} + \mathcal{L} \right], \tag{3}$$

where $dM = \sqrt{-g}d^4x$ is the invariant volume element, M is the 4D spacetime manifold, $R = R^\mu_\mu = g^{\mu\nu}R_{\mu\nu}$ the Ricci scalar curvature and $\mathcal{L}$ the Lagrangian of the energy-matter content. We can obtain Einstein's field equations (EFE) for the metric field $g_{\mu\nu}$ from this action by requiring S to be stationary $\delta S = 0$ under arbitrary variations of the metric $\delta g^{\mu\nu}$. The solution is (Einstein 1916; Weinberg 2008; Padmanabhan 2010):

$$G_{\mu\nu} + \Lambda g_{\mu\nu} = 8\pi G\, T_{\mu\nu} \equiv -\frac{16\pi G}{\sqrt{-g}} \frac{\delta(\sqrt{-g}\mathcal{L})}{\delta g^{\mu\nu}}, \tag{4}$$

where $G_{\mu\nu} \equiv R_{\mu\nu} - \frac{1}{2}g_{\mu\nu}R$ and $\mathcal{L}$ is the matter Lagrangian. For perfect fluid in spherical coordinates:

$$T_{\mu\nu} = (\rho + p)u_\mu u_\nu + p g_{\mu\nu} \tag{5}$$

where u_ν is the 4-velocity ($u_\nu u^\nu = -1$), ρ, and p are the energy-matter density and pressure. This fluid is in general made of several components, each with a different equation of state $p = \omega\rho$. In general, for a fluid moving with relative radial velocity u with $u^\nu = (u^0, u, 0, 0)$, we have $u_0^2 = -g_{00}(1 + g_{11}u^2)$ and:

$$T^0_0 = -\rho - u^2(\rho + p)g_{11} \quad ; \quad T^1_1 = p + u^2(\rho + p)g_{11}$$
$$T^1_0 = (\rho + p)\, u_0 u \quad ; \quad T^2_2 = T^3_3 = p \tag{6}$$

For a comoving observer $u = 0$. The outside manyfold $\mathcal{M}_+$ is empty space so the outside netric g_+ is the BH.SW. Because the inside $\mathcal{M}_-$ is causally disconnected, $\mathcal{M}_+$ acts like a boundary condition (Gaztañaga 2021). Given some ρ and p inside r_{SW}, we will solve EFE inside to find g_-. To impose the boundary at r_{SW} we will use the same (physical) SW outside coordinate frame (that is not comoving with the fluid). This will result in solutions for $\mathcal{M}_-$ that are not static. We will the verify Israel's conditions (Israel 1967) to check that the join manyfold $\mathcal{M} = \mathcal{M}_- \cup \mathcal{M}_+$ is also a solution to EFE without any surface terms (see §3.4).

It turns out that for a perfect fluid the solution that minimizes the action results in a boundary term for the minimum action (on-shell) Gaztañaga (2021):

$$S^{on-sh} = \int_M dM \frac{\nabla_\mu \mathsf{g}^\mu}{8\pi G} = \oint_{\partial M} \frac{dV_\mu \mathsf{g}^\mu}{8\pi G} = < \Lambda/4\pi G - (\rho + 3p) >_M$$

(7)

where in the last step we have used Raychaudhuri equation (Eq.53) and the average is over the lightcone in M bounded by ∂M, which we defined by a causal boundary: $\chi < \chi_\S$. If we want this boundary to vanish, so that the action is zero in empty space, we need $S^{on-sh} = 0$. For $\chi_\S = \infty$ this means $\Lambda = 0$. The observational fact that $\Lambda \neq 0$ implies that $\chi_\S$ is finite. This boundary term condition is basically the same as the $r_\Lambda = r_{SW}$ boundary in the solutions we will present in §3.

2.1 Scalar field in curved space-time

Consider a minimally coupled scalar field $\varphi = \varphi(x_\alpha)$ with:

$$\mathcal{L} \equiv K - V = -\frac{1}{2}\partial_\alpha\varphi\partial^\alpha\varphi - V(\varphi) \tag{8}$$

The Lagrange equations are: $\bar{\nabla}^2\varphi = \partial V/\partial\varphi$. We can estimate $T_{\mu\nu}(\varphi)$ from its definition in Eq.4 to find Weinberg (2008):

$$T_{\mu\nu}(\varphi) = \partial_\mu\varphi\partial_\nu\varphi + g_{\mu\nu}(K - V) \tag{9}$$

comparing to Eq.5:

$$\rho = K + V \quad ; \quad p = |K| - V \tag{10}$$

In general we can have $p_\parallel \neq p_\perp$ for non canonical scalar fields (see Eq.5 in Diez-Tejedor & Feinstein (2006) for further details). The stable solution corresponds to $p = -\rho \equiv -\rho_{vac}$:

$$\bar{\nabla}^2\varphi = \partial V/\partial\varphi = 0 \quad ; \quad \rho \equiv \rho_{vac} = -p = V(\varphi) = V_i \tag{11}$$

where φ is trapped in the true minimum V_0 or some false vacuum (FV) state $V_i = V_0 + \Delta$. The situation is illustrated in Fig.1. Consider a localized field with some fixed total energy $\rho = K + V$ (black dot labeled ρ_5 in the figure). In an expanding background (such a supernovae explosion or Inflation) the field can rapidly lose its kinetic energy (K_5), due to Hubble damping, and end up trapped inside some FV (V_5). If the outside background is at a lower FV, this will generate an expanding BH of type BH.fv, as we will discuss in §3.2. This could be the final outcome of stellar collapse, or the start of some new cosmic inflation, avoiding the traditional BB or BH.SW singularities. Because additional FV structure can exist within a given FV, the same Hubble damping can form a BH.fv inside a larger BH.fv. When K is not fully damped, the classical reheating mechanism around a FV could also be a source of matter/radiation. This could turn a BH.fv into BH.u (see §3.3). Quantum tunnelling can result in a phase transition or vacuum evaporation, which can also be a source of matter/radiation and new BH.fv.

2.2 The FLRW metric in comoving coordinates

The FLRW metric in comoving coordinates $\xi^\alpha = (\tau, \chi, \delta, \theta)$, corresponds to an homogeneous and isotropic space:

$$ds^2 = f_{\alpha\beta}d\xi^\alpha d\xi^\beta = -d\tau^2 + a(\tau)^2\left[d\chi^2 + \chi^2 d\omega_k^2\right] \tag{12}$$

where we have introduced the solid angle: $d\omega_k \equiv \mathrm{sinc}(\sqrt{k}\chi)d\omega$ with $d\omega^2 = \cos^2\delta d\theta^2 + d\delta^2$ and k is the curvature constant $k = \{+1, 0, -1\}$. For the flat case ($k = 0$) we have $d\omega_k^2 = d\omega^2$. The scale factor, $a(\tau)$, describes the expansion/contraction as a function of comoving or cosmic time τ (proper time for a comoving observer). For a comoving observer, the time-radial components are:

$$\begin{pmatrix} T_{00} & T_{10} \\ T_{01} & T_{11} \end{pmatrix} = \begin{pmatrix} \rho(\tau) & 0 \\ 0 & p(\tau)a^2 \end{pmatrix} \tag{13}$$

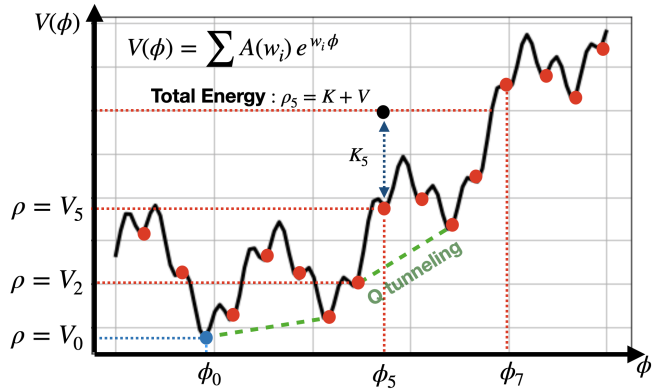

Figure 1. The potential $V(\phi)$, of a classical scalar field $\phi(x)$, made of the superposition of plane waves. A configuration with total energy: $\rho_5 = K_5 + V_5$ (black dot at ϕ_5) can loose its kinetic energy K_5 during expansion (e.g. a supernova explosion or a expanding background) due to Hubble damping and relax into one of the static ($K = 0$) ground state (or FV) $\rho_5 = V_5 \equiv V(\phi_5)$ (red dots). This can generate a Black Hole (BH.fv) and regular matter from reheating. Each FV has an energy excess $\Delta_i \equiv V_i - V_0$ over the true vacuum at V_0 (blue dot). Quantum tunneling (dashed lines) could allow ϕ to jump between FV, resulting in BH evaporation and new matter/radiation.

i.e. $u = 0$ in Eq.6. The solution to EFE in Eq.4 is:

$$3\left(\frac{\ddot{a}}{a}\right) = R_{\mu\nu}u^\mu u^\nu = \Lambda - 4\pi G(\rho + 3p) \tag{14}$$

$$H^2 \equiv \left(\frac{\dot{a}}{a}\right)^2 = H_0^2\left[\Omega_m a^{-3} + \Omega_R a^{-4} + \Omega_k a^{-2} + \Omega_\Lambda\right] \tag{15}$$

$$\rho_\Lambda \equiv \rho_{\rm vac} + \frac{\Lambda}{8\pi G} \tag{16}$$

$$\rho_c \equiv \frac{3H^2}{8\pi G} \quad ; \quad \Omega_X \equiv \frac{\rho_X}{\rho_c(a=1)} \tag{17}$$

where Ω_m (or ρ_m) represent the matter density today ($a = 1$), Ω_R is the radiation, $\rho_{\rm vac}$ represents vacuum energy: $\rho_{\rm vac} = -p_{\rm vac} = V(\varphi)$ in Eq.11, and $\rho_\Lambda = -p_\Lambda$ is the effective cosmological constant density. Note that Λ (the raw value) is always constant, but ρ_Λ (effective value) can change if ρ_{vac} changes. Given ρ and p at some time, we can use the above equations to find $a = a(\tau)$ and determine the metric in Eq.12.

2.3 The FLRW metric as a Black Hole

Observations show that the expansion rate today is dominated by ρ_Λ. This indicates that the FLRW metric lives inside a trapped surface $r_\Lambda \equiv 1/H_\Lambda = (8\pi G\rho_\Lambda/3)^{-1/2}$, which behaves like the interior of a BH. To see this, consider outgoing radial null geodesic (the Event Horizon at τ, Ellis & Rothman 1993):

$$r_* \equiv a\chi_* = a(\tau)\int_\tau^\infty \frac{d\tau}{a(\tau)} = a\int_a^\infty \frac{d\ln a}{aH(a)} < \frac{1}{H_\Lambda} \equiv r_\Lambda \tag{18}$$

where χ_* is the corresponding comoving scale. This is shown as a red dashed line in Fig.2. We can see that such Event Horizon is constant, χ_*, in comoving coordinates for $a < 1$ and becomes fixed in physical coordinates to $r_* = r_\Lambda$ for $a > 1$. No signal from inside r_* can reach outside, just like in the interior of a BH. In fact, according to Birkhoff theorem (see Deser & Franklin 2005), the metric outside should be exactly that of the BH.SW if we approximate that such space is empty (as we do for regular SW BH). So the FLRW metric is a

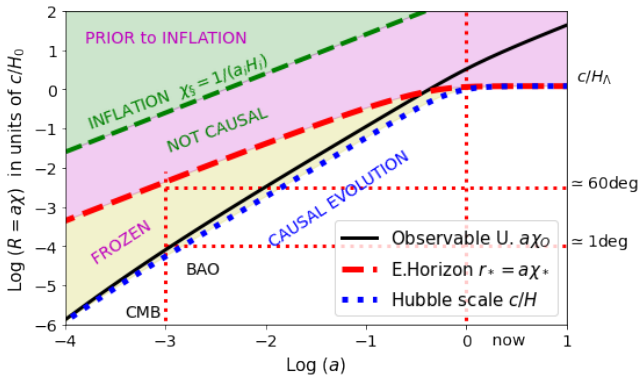

Figure 2. Physical radial coordinate $R = a(\tau)\chi$ in units of c/H_0 as a function of cosmic time a for a flat $\Omega_\Lambda = 0.75$ FLRW metric. The Hubble horizon c/H (blue dotted line), is compared to the observable universe r_o in Eq.19 (black continuous line) and the FLRW Event Horizon $r_* = a\chi_*$ in Eq.18 (red dashed line), which here is smaller than the primordial causal boundary for inflation $\chi_§$ (green dashed line). Scales larger than r_* are causally disconnected (magenta shading) while scales larger than $a\chi_§$ are prior to inflation. Scales smaller than r_* but larger than c/H are dynamically frozen (yellow shading). At $a \simeq 1$ (close to now) the Hubble horizon reaches our event horizon $a\chi_* = c/H_\Lambda$. Table 1 gives a summary of the different scales presented.

BH:SW from the outside with $r_{SW} = r_\Lambda$. This breaks homogeneity (on scales larger than r_Λ), but this is needed if we want causality. Homogeneity is strickly inconsistent with a causal origin.

The causal boundary of inflation $\chi_§$ (shown as green dashed line) corresponds to the particle horizon during inflation $\chi_§ = c/(a_i H_i)$ or the Hubble horizon $1/H_i$ when inflation begins a_i. We can in princile have that $\chi_§ > \chi_*$, as shown in the figure. But why should there be two separate causal scales? We will argue below that is natural to assume that our Event Horizon χ_* and the primordial causal boundary $\chi_§$ are the same: $\chi_§ = \chi_*$, which provides a fundamental explanation for the measured effective Λ.

The observable universe (particle horizon or past null cone) after inflation in comoving coordinates is:

$$r_o = a\chi_o = a\chi_o(a) = a\int_{a_e}^{a} \frac{d\ln a}{aH(a)} \tag{19}$$

where a_e is the scale factor when inflation ends. For $\Omega_\Lambda \simeq 0.7$, the particle horizon today is $r_o \simeq 3.26c/H_0$, which is larger than r_Λ as shown in Fig.2. This shows that, observers like us are trapped inside $r_* = a\chi_*$ but can nevertheless observe what happened outside. If we look back to the CMB maps ($a \simeq 10^3$) we can see frozen BAO scales (outsisde the Hubble scale $1/H$ at $\theta \simeq 1$deg. on the sky) but also scales outside our Event Horizon r_* ($\theta \simeq 60$deg. on the CMB sky).

2.4 Spherical symmetry in physical coordinates

The most general shape for a metric with spherical symmetry in physical or SW coordinates (t, r, δ, θ) is (Padmanabhan 2010):

$$ds^2 = g_{\mu\nu}dx^\mu dx^\nu = -(1+2\Psi)dt^2 + \frac{dr^2}{1+2\Phi} + r^2 d\omega_k^2 \tag{20}$$

where $d\omega_k$ was introduced in Eq.12 to allow for non-flat space. $\Psi(t,r)$ and $\Phi(t,r)$ are the two gravitational potentials. The Weyl potential Φ_W is the geometric mean of the two:

$$(1+2\Phi_W)^2 = (1+2\Phi)(1+2\Psi) \tag{21}$$

Ψ describes propagation of non-relativist particles and Φ_W the propagation of light. For $p = -\rho$ we have $\Psi = \Phi = \Phi_W$. Eq.20 can also be used to describe the BH.SW solution (or any other solution) as a perturbation ($2|\Phi| < 1$) around a FLRW background:

$$ds^2 \simeq -(1+2\Psi)dt^2 + (1-2\Phi)a^2 d\chi^2 + a^2\chi^2 d\omega_k^2 \tag{22}$$

where $r = a(\tau)\chi$ and $t \simeq \tau$. The same result follows from perturbing the FLRW metric in Eq.12.

Solutions to EFE for Eq.20 are well known, e.g. see Eq.(7.51) in Padmanabhan (2010). For a static perfect fluid with arbitrary $\rho(r)$ inside r_{SW} and empty space ($\Lambda = 0$) outside, we have $G_0^0 = -8\pi G\rho(r)$. This can be solved using $m(r) \equiv \int_0^r \rho(r)\, 4\pi r^2 dr$:

$$\Phi(r) = -\frac{Gm(r)}{r} = \begin{cases} -GM/r & \text{for } \rho(r) = M\,\delta_D(r) \\ -\frac{1}{2}(r/r_0)^2 & \text{for } \rho(r) = \rho_0 \equiv \frac{3}{8\pi r_0^2} \end{cases} \tag{23}$$

$\Psi(r)$ depends on G_1^1 and $p(r)$. For $p = -\rho$ we have $G_0^0 = G_1^1$ and the general solution with $\Lambda \neq 0$ is:

$$\Phi = \Psi = -\frac{Gm(r)}{r} - \frac{\Lambda r^2}{6} \tag{24}$$

The remaining EFE, $G_2^2 = G_3^3$ correspond to energy conservation $\nabla_\mu T_\nu^\mu = 0$. For a comoving observer $u = 0$ in a perfect fluid of Eq.6:

$$\partial_t \rho = -\frac{\rho + p}{1+2\Phi}\,\partial_t \Phi. \;\; ; \;\; \partial_r p = \frac{\rho + p}{1+2\Psi}\,\partial_r \Psi \tag{25}$$

Note how $\rho = -p$ results in constant ρ and p everywhere, but with a discontinuity at $2\Phi = 2\Psi = -1$. This means that ρ and p can be constant, but different in both sides of $2\Phi = 2\Psi = -1$. This can be addressed with the study of junction conditions (see §3.4). We can also consider anisotropic pressure $p_\parallel \neq p_\perp$ (Brustein & Medved 2019; Dymnikova 2019) which can result from non canonical scalar field (Diez-Tejedor & Feinstein 2006). Empty space ($\rho = p = \rho_\Lambda = 0$) in Eq.24 results in the BH.SW metric:

$$2\Phi = 2\Psi = -2GM/r \equiv -r_{SW}/r \tag{26}$$

There is a trapped surface at $r = r_{SW}$ ($2\Phi = -1$). Outgoing radial null geodesics cannot leave the interior of r_{SW}, while incoming ones can cross inside. The solution to Eq.24 for $\rho = p = M = 0$, but $\rho_\Lambda \neq 0$ results in deSitter (dS) metric:

$$2\Phi = 2\Psi = -r^2/r_\Lambda^2 \equiv -r^2 H_\Lambda^2 = -r^2 8\pi G\rho_\Lambda/3 \tag{27}$$

where ρ_Λ is the effective density: $\rho_\Lambda = \Lambda/(8\pi G) + V(\varphi)$. We can immediately see that this solution is the same as the interior of a BH with constant density in Eq.23 with $\rho_0 = \rho_\Lambda$. Topologically, dS metric corresponds to the surface of a hypersphere of radius r_Λ in a flat spacetime with an extra spatial dimension (see Appendix A). As in the BH.SW metric, dS metric also has a trapped surface at $r = r_\Lambda$ ($2\Phi = -1$). Radial null events ($ds^2 = 0$) connecting $(0, r_0)$ with (t, r) follow:

$$r = r_\Lambda \frac{r_\Lambda + r_0 - (r_\Lambda - r_0)e^{-2t/r_\Lambda}}{r_\Lambda + r_0 + (r_\Lambda - r_0)e^{-2t/r_\Lambda}} \tag{28}$$

so that it takes $t = \infty$ to reach $r = r_\Lambda$ from any point inside. The BH.SW metric is singular at $r = 0$, while dS is singular at $r = \infty$. In comoving coordinates, dS singularity corresponds to a comoving Hubble horizon that shrinks to zero (see Fig.5). But note that this singularity can not be reached from the inside because of the trapped surface at r_Λ in Eq.28. The inside observer is trapped, also like in the FLRW case. In fact, both metrics are equivalent for $H = H_\Lambda$ (see Lanczos 1922; Mitra 2012) which explains why the dS metric reproduces primordial inflation in comoving coordinates.

Table 1. Some notation used in this paper.

Notation	name	comment
$-2\Phi = r_{SW}/r$	SW = Schwarzschild Eq.26	BH.SW, outside BHU
$-2\Phi = r^2/r_\Lambda^2$	dS = deSitter Eq.27	static, inside BH.fv
$-2\Phi = r^2/r_H^2$	dSE= dS Extension Eq.29	FLRW, inside BH.u
$-2\Phi = r_{SW}/r + r^2/r_\Lambda^2$	dSW = dS-SW	static, outside BHU
$r_\Lambda \equiv 1/H_\Lambda$	dS Event Horizon	$3H_\Lambda^2 = 8\pi G\rho_\Lambda$, Eq.27
$r_{SW} \equiv 2GM$	BH Event Horizon	$\rho_{BH}(r_\Lambda) = \rho_\Lambda$, Eq.1
$r_* \equiv a\chi_* = a\int_\tau^\infty \frac{d\tau}{a(\tau)}$	FLRW Event Horizon	Outgoing null geodesics Eq.18
$r_o \equiv a\chi_o = a\int_0^\tau \frac{d\tau}{a(\tau)}$	Observable Universe	Particle Horizon Eq.19
$r_H(\tau) \equiv 1/H(\tau)$	Hubble Horizon	$r > r_H$ frozen Fig.2
$R = (r_H^2 r_{SW})^{1/3}$	BH Junction Eq.48	$R = r_\Lambda = r_{SW}$ Eq.44
$r_\S \equiv a(\tau)\chi_\S$	Causal Boundary Eq.7,54	for Inflation: $\chi_\S = \frac{1}{a_i H_i}$

As first noticed by Einstein (O'Raifeartaigh & Mitton 2015), the Steady-State Cosmology (SSC), with a perfect cosmological principle, is also reproduced by dS metric. But contrary to the original SSC proposal of Bondi & Gold (1948); Hoyle (1948), there is no need for continuous matter creation (or a C-field) because the metric is expanding in comoving coordinates but is static in physical coordinates because $\rho_\Lambda = V(\varphi)$ is trapped to a fixed FV value in Eq.11.

We will also consider a generalization of dS metric, which we call dS extension (dSE), which is just a recast of the general case:

$$2\Phi(t,r) \equiv -r^2H^2(t,r) \equiv -r^2/r_H^2 \tag{29}$$

where $r_H \equiv 1/H$ corresponds to the Hubble radius. Table 1 shows a summary of notation and metrics considered in this paper. When we have both M and ρ_Λ constant, the solution to Eq.24 is: $2\Phi = 2\Psi = -r^2H_\Lambda^2 - r_{SW}/r$, which corresponds to dS-SW (dSW) metric, a BH.SW within a dS background. Solution of a BH inside a FLRW metric also exist (e.g see Kaloper et al. 2010). Here we will show that GR solutions also exit for a FLRW inside a BH (or inside a larger FLRW metric).

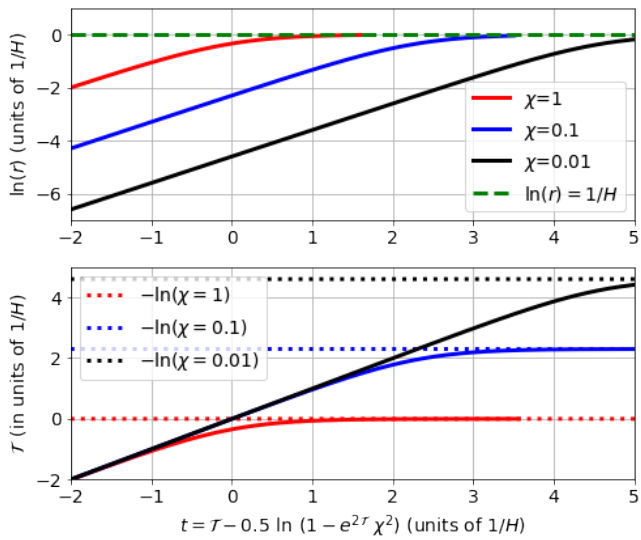

Figure 3. Logarithm of physical radius $r = a(\tau)\chi$ (top) and comoving time τ (bottom) as a function of SW time t in Eq.33 for $a(\tau) = e^{\tau H_\Lambda}$ and different values of χ. All quantities are in units of $1/H_\Lambda$. For early time or small χ: $\tau \simeq t$. A fix χ acts like an Horizon: as $t \Rightarrow \infty$ we have $\tau \Rightarrow -\ln\chi$ (dotted), which freezes inflation to: $r = a\chi \Rightarrow e^{-\ln(H_\Lambda\chi)}\chi = 1/H_\Lambda$ (dashed).

3 SOME NEW SOLUTIONS

3.1 The FLRW metric in physical coordinates

Consider a change of variables from $x^\mu = [t, r]$ to comoving coordinates $\xi^\nu = [\tau, \chi]$, where $r = a(\tau)\chi$ and angular variables (δ, θ) remain the same. The metric $g_{\mu\nu}$ in Eq.20 transforms to $f_{\alpha\beta} = \Lambda^\mu_\alpha \Lambda^\nu_\beta g_{\mu\nu}$, with $\Lambda^\mu_\nu \equiv \frac{\partial x^\mu}{\partial \xi^\nu}$. If we use:

$$\Lambda = \begin{pmatrix} \partial_\tau t & \partial_\chi t \\ \partial_\tau r & \partial_\chi r \end{pmatrix} = \begin{pmatrix} (1+2\Phi_W)^{-1} & arH(1+2\Phi_W)^{-1} \\ rH & a \end{pmatrix}, \tag{30}$$

with $2\Phi = -r^2H^2$ and arbitrary $a(\tau)$ and Ψ, we find:

$$f_{\alpha\beta} = \Lambda^T \begin{pmatrix} -(1+2\Psi) & 0 \\ 0 & (1+2\Phi)^{-1} \end{pmatrix} \Lambda = \begin{pmatrix} -1 & 0 \\ 0 & a^2 \end{pmatrix}, \tag{31}$$

In other words, these two metrics are the same:

$$-(1+2\Psi)dt^2 + \frac{dr^2}{1-r^2H^2} + r^2 d\omega_k^2 = -d\tau^2 + a^2\left[d\chi^2 + \chi^2 d\omega_k^2\right] \tag{32}$$

dSE metric of Eq.29: $2\Phi = -r^2H^2$ corresponds to the FLRW metric with $H(t,r) = H(\tau)$: this is a hypersphere of radius r_H that tends to r_Λ (see Appendix A). This frame duality can be understood as a Lorentz contraction $\gamma = 1/\sqrt{1-u^2}$ where the velocity u is given by the Hubble-Lemaitre law: $u = Hr$. The SW frame, that is not moving with the fluid, sees a moving fluid element $ad\chi$ contracted by the Lorentz factor γ: $ad\chi \Rightarrow \gamma dr$. For constant H, the FLRW metric corresponds the interior of a BH with constant density in Eq.23. A Lorentz factor γ also explains $d\tau = \gamma^{-1}dt$ as time dilation.

In general, we can find $\Psi = \Psi(t,r)$ and $t = t(\tau,\chi)$ or $\tau = \tau(t,r)$ given $a(\tau)$. For $a(\tau) = e^{\tau H_\Lambda}$ we have $2\Psi = 2\Phi = -r^2H_\Lambda^2$ and (see Lanczos 1922; Lanczos & Hoenselaers 1997):

$$t = t(\tau,\chi) = \tau - \frac{1}{2H_\Lambda}\ln\left[1 - H_\Lambda^2 a^2\chi^2\right], \tag{33}$$

where $r < r_\Lambda = 1/H_\Lambda$, which reproduces dS metric. In comoving coordinates the metric is inflating exponentially: $a = e^{\tau H_\Lambda}$, while in physical coordinates it is static. Fig.3 illustrates how this is possible and shows how $\tau = \tau(t,r)$ freezes (see Mitra 2012 for some additional discussion). Note also how $\partial_\tau t = (1+2\Phi_W)^{-1}$ in Eq.30 for $2\Phi_W = -r^2H^2$ is the generalization of Eq.33 for $\dot{H} \neq 0$. The general frame duality of Eq.32, from a comoving frame to a physical SW frame, is a new result as far as we know, and a key ingredient to interpret our new physical BH solutions.

3.2 False Vacuum Black Hole (BH.fv) solution

Eq.26 and Eq.27 are the simplest solutions to EFE. They correspond to some form of empty space. The simplest modeling of physical BH interior is a combination of the two (see Eq.2.2 in Blau et al. 1987):

$$\rho = -p = \begin{cases} 0 & \text{for } r > r_{SW} \\ \Delta & \text{for } r < r_{SW} \end{cases} \tag{34}$$

where $\Delta > 0$. To recover the BH.SW solution outside, we use $V_0 = \Lambda_+ = 0$. In a more realistic situation, on larger scales the BH.SW metric should be considered a perturbation of FLRW background, e.g. Eq.22, with $\Lambda_+ \neq 0$ and $V_0 \neq 0$, in fact we could also have a FLRW metric outside (see Appendix B). The solution to EFE in Eq.24 for Eq.34 (which we called BH.fv) is then:

$$2\Phi = 2\Psi = \begin{cases} -r_{SW}/r & \text{for } r > r_{SW} \equiv 2GM \\ -r^2 H_{\Lambda_-}^2 & \text{for } r < r_{SW} = r_{\Lambda_-} \equiv 1/H_{\Lambda_-} \end{cases} \tag{35}$$

where: $\rho_{\Lambda_-} = \rho_{BH} = \Delta$ and $M = \frac{4\pi}{3} r_{SW}^3 \Delta$. Recall that $\Lambda = V_0 = 0$ and ρ_{Λ_-} refers to the effective Λ density inside the BH. The above solution has no singularity at $r = 0$. Note how, contrary to what happens in the BH.SW, in the BH.fv solution, the metric components don't change signature as we cross inside r_{SW}. In both sides of r_{SW} we have constant but different values of p and ρ. This comes from energy conservation in Eq.25. There is a discontinuity at $2\Phi = -1$ where $r = r_{SW}$, in agreement with Eq.25, but the metric is static and continuous at r_{SW}. This solution only happens when $r_{SW} = r_{\Lambda_-} = (8\pi G\Delta/3)^{-1/2}$. The smaller Δ the larger and more massive the BH. In the limit $\Delta \Rightarrow 0$, we have $r_{SW} = r_{\Lambda_-} \Rightarrow \infty$ and we recover Minkowski space, as expected.

At a fixed location, the scalar field φ inside the BH is trapped in a stable configuration ($\rho = V_0 + \Delta$) and can not evolve ($K = 0$ in Eq.10). The same happens for the field outside (see Fig.1). A FV in Eq.34 with equal Δ but with smaller initial radius $r = R < r_{SW}$ is subject to a pressure discontinuity at $r = R$ which is not balanced in Eq.25 and results in a bubble growth (Blau et al. 1987; Aguirre & Johnson 2005). Such boundary grows and asymptotically reaches $R = r_{SW}$ (see top panel of Fig.3 and Eq.51). The inside of r_{SW} is causally disconnected, so the pressure discontinuity does not act on $r = r_{SW}$, which corresponds to a trapped surface.

3.3 Black Hole Universe (BH.u) solution

We next look for solutions where we have matter $\rho_m = \rho_m(t, r)$ and radiation $\rho_R = \rho_R(t, r)$ inside but an empty BH.SW outside:

$$\rho(t, r) \quad = \quad \begin{cases} -p = 0 & \text{for } r > r_{SW} \\ \Delta + \rho_m + \rho_R & \text{for } r < r_{SW} \end{cases} . \tag{36}$$

Note that $p = -\Delta + \rho_R/3 \neq -\rho$ inside, so that $\partial_t \Phi \neq 0$ and $u \neq 0$: the fluid inside has to move relative to SW frame of the outside observer. For $r > r_{SW}$, the solution is the same as Eq.35. For the interior we use the dSE notation in Eq29: $2\Phi(t, r) \equiv -r^2 H^2(t, r)$, so that:

$$2\Phi(t, r) = \begin{cases} -r_{SW}/r & \text{for } r > r_{SW} = 2GM \\ -r^2 H^2(t, r) & \text{for } r < r_{SW} = r_H \end{cases} \tag{37}$$

Note how the interior Event Horizon $2\Phi = -1$ corresponds to $r = r_H \equiv 1/H$, which is not fixed in (t, r) coordinates, while r_Λ is fixed. But note that r_H asymptotically tends to r_Λ from below. We will study this junction in more detailed in §3.4.2.

We can find the interior solution with a change of variables of Eq.30-32. This converts dSE metric into FLRW metric so the solution is just $H(t, r) = H(\tau)$. Given ρ and p in the interior of a BH we can use Eq.15 with $\rho_{\Lambda_-} = \Delta = 3r_{SW}^{-2}/8\pi G$ to find $H(\tau)$ and $a(\tau)$. We call this a BH universe (BH.u). To complete the solution, i.e. to find Ψ and $\tau = \tau(t, r)$, we need to solve Eq.30 with $2\Phi = -r^2 H^2(\tau)$. For $H(\tau) = H_{\Lambda_-}$ the solution is $\Psi = \Phi$ and Eq.33. The flat FLRW metric with $H = H_{\Lambda_-}$ becomes dS metric in Eq.27 as in the BH.fv solution.

Given $T_{\mu\nu}$ in Eq.13 we can find $\bar{T}_{\alpha\beta}$ in the physical SW frame using the inverse matrix of Eq.30: $\bar{T}_{\alpha\beta} = (\Lambda^{-1})^\mu_\alpha (\Lambda^{-1})^\nu_\beta T_{\mu\nu}$:

$$\bar{T}_0^0 = -\frac{\rho - p2\Phi}{1 + 2\Phi} \;\; ; \;\; \bar{T}_1^1 = \frac{p - \rho 2\Phi}{1 + 2\Phi} \tag{38}$$

which is independent of Ψ. Comparing to Eq.6 gives the velocity in the physical SW frame $u^2 = -2\Phi = r^2 H^2$, which is just the Hubble-Lemaitre law. The Lorentz factor is $\gamma = (1 + 2\Phi)^{-1/2}$ so that γdr gives the physical SW length, in agreement with Eq.20.

Solution $H(t, r) = H(\tau)$ in Eq.37 is valid for all $r < r_{SW} = 1/H_{\Lambda_-}$ because $H(\tau) > H_{\Lambda_-}$. We can see this by considering outgoing radial null geodesic in the FLRW metric of Eq.18. which shows that signals can not escape from the inside to the outside of the BH.u. But incoming radial null geodesics Eq.19 can in fact be larger than r_{SW} if we look back in time. This shows that inside observers are trapped inside the BH.u but they can nevertheless observe what happened outside (Gaztañaga & Fosalba 2021).

3.4 Junction conditions

We can arrive at the same BHU (BH.fv and BH.u) solutions using Israel's junction conditions (Israel 1967). Here we follow closely the notation in §12.5 of Padmanabhan (2010). We will combine two solutions to EFE with different energy content, as in Eq.36, on two sides of a hypersurface $\Sigma = \mathcal{M}_- \cap \mathcal{M}_+$. The inside g_- is FLRW metric (or dS metric for $H = H_\Lambda$) and the outside g_+ is BH.SW metric. The junction conditions require that the metric and its derivative (the extrinsic curvature K) match at Σ. This means that the join metric provides a new solution to EFE in the joined manyfold $\mathcal{M} = \mathcal{M}_- \cup \mathcal{M}_+$. In many cases, like in the Bubble Universes, this does not work and the junction requires a surface term (the bubble) to glue both solutions together. This is not the case here. We will show that in the limit of large or small times (or scale factor a) the junction conditions are satisfied and there are no surface terms.

The effective Λ term corresponds to a trapped surface $r_{SW} = 1/H_{\Lambda_-}$ in the FLRW (or dS) metric which matches the horizon of a BH in empty space (see Fig.6). In a more realistic case, the external background is not empty and we then need to study the junction of two FLRW with two different effective Λ_- and Λ_+, different matter content and different Hubble-Lemaitre laws $a(\tau)$. The effective Λ_- will be the trapped surface of a BH inside the outside FLRW metric. Here we just want to point out that such solutions exist and more work is needed to workout more realistic situations. In what follows, for easy of notation, we will use $\Lambda = \Lambda_-$ (i.e., $\rho_\Lambda = \rho_{\Lambda_-}$) and assume that $\rho_+ = 0$, which is what is usually done for a SW BH. But this can be trivially generalized to $\rho_{\Lambda_+} \neq 0$ (e.g. see Appendix B).

3.4.1 Null junction

As we want Σ to correspond to a causal horizon we choose Σ to be a radial null surface in the FLRW metric, i.e.: $d\tau = a d\chi$. This results in a radial coordinate $\chi_*(\tau)$ which we want to identify with the FLRW event horizon of Eq.18. At any given time the corresponding physical distance is $r_*(\tau) = a\chi_*$. For the outside SW coordinate system, Σ_+ is described by $r = R(\tau)$ and $t = T(\tau)$, where τ is the comoving time in the FLRW metric. We then have:

$$dr = \dot{R} d\tau \;\; ; \;\; dt = \dot{T} d\tau, \tag{39}$$

where the dot refers to derivatives with respect to τ. The induced metric h_- on the inside of Σ_- with $y^a = (\tau, \delta, \theta)$ and $d\tau = a d\chi$ is:

$$ds^2_{\Sigma_-} = h_{ab} dy^a dy^b = r_*^2 d\omega^2 \tag{40}$$

This has to agree with h_+, the BH.SW metric outside at Σ_+:

$$-F dt^2 + F^{-1} dr^2 + r^2 d\omega^2 = -(F\dot{T}^2 - \dot{R}^2/F) d\tau^2 + R^2 d\omega^2 \tag{41}$$

where $F \equiv 1 - r_{SW}/R$. The first matching condition $h_- = h_+$ is:

$$R(\tau) = r_*(\tau) \;\; ; \;\; F^2 \dot{T}^2 = \dot{R}^2 \tag{42}$$

Thus, for a given FLRW solution $a(\tau)$ we know both R and β. We next estimate the extrinsic curvature $K^\pm$ normal to $\Sigma_\pm$ from each side. The outward normal to Σ on the inside is $n^- = (-1, -a, 0, 0)$ and on the outside $n^+ = (-\dot{R}, \dot{T}, 0, 0)$. Using the corresponding 4D Christoffel symbols $\Gamma_\pm$, we find:

$$\begin{aligned}
K^-_{\tau\tau} &= \nabla^-_\tau n^-_\tau = 0 \\
K^+_{\tau\tau} &= \dot{T}\Gamma^r_{+tt} = \dot{T} F \frac{1-F}{2R} \\
K^-_{\theta\theta} &= (-\Gamma^\tau_{-\theta\theta} - a\Gamma^\chi_{-\theta\theta}) = -r_*(Hr_* - 1) \\
K^+_{\theta\theta} &= \dot{T}\,\Gamma^r_{+\theta\theta} = \dot{T}\,(r_{SW} - R) = -\dot{T} F R \\
K^\pm_{\delta\delta} &= \sin^2\theta\, K^\pm_{\theta\theta}
\end{aligned} \tag{43}$$

The matching condition $K^- = K^+$ together with Eq.42 results in:

$$\dot{r}_* = 0 \qquad \& \qquad R = r_* = r_{SW} = r_H \tag{44}$$

This results in $2\Psi = 2\Phi = -H^2R^2 = -r_{SW}/R = 1$ in the junction Σ, as in Eq.37. But this solution is only valid for constant $H = H_\Lambda$ (or $\dot{r}_H = 0$) so in the limit of the BH.fv solution in Eq.35. This makes sense because for a dS expansion null events are fixed in physical coordinates. This happens for $a > 1$ in Fig.2. But as noted in Eq.18 the FLRW event horizon r_* becomes constant in comoving coordinates for $a < 1$. We will explore this junction case next.

3.4.2 Timelike Junction

Here we will consider a situation where ρ_Λ is negligible. As shown by Eq.18 and Fig.2 the FLRW event horizon is then fixed in comoving coordinates. This corresponds to an earlier time in our universe (dominated by matter or radiation) or to universe or a BH without a FV. We choose Σ to be fixed in comoving coordinates at χ_{SW}, so that Σ is timelike and only depends τ. Here we define $a = 1$ when $\chi_{SW} = r_{SW}$. Note how this is different from the standard notation in Eq.15 which fixes $a = 1$ to now. For the outside SW coordinate system, Σ_+ is described by $r = R(\tau)$ and $t = T(\tau)$, where τ is the comoving time in the FLRW metric as before in Eq.39. The induced metric h_- on the inside of Σ_- with $y^a = (\tau, \delta, \theta)$ and fixed $\chi = \chi_{SW}$, is now different from Eq.40:

$$ds^2_\Sigma = h_{ab} dy^a dy^b = -d\tau^2 + a^2(\tau)\chi^2_{SW} d\omega^2 \tag{45}$$

This has to agree with the h_+, the BH.SW metric outside at Σ_+ in Eq.41. The first matching condition $h_- = h_+$ is now:

$$R(\tau) = a(\tau)\chi_{SW} \;\; ; \;\; F\dot{T} = \sqrt{\dot{R}^2 + F} \equiv \beta(R, \dot{R}) \tag{46}$$

For a given FLRW solution $a(\tau)$ we know both R and β. The extrinsic curvature is now:

$$\begin{aligned}
K^\tau_{-\tau} = 0 \;\; &; \;\; K^\theta_{-\theta} = K^\delta_{-\delta} = -\frac{1}{a\chi_{SW}} \\
K^\tau_{+\tau} = \frac{\dot{\beta}}{\dot{R}} \;\; &; \;\; K^\theta_{+\theta} = K^\delta_{+\delta} = -\frac{\beta}{R}
\end{aligned} \tag{47}$$

Thus, the second matching condition $K_- = K_+$ requires $\beta = 1$, which using Eq.46 results in:

$$\dot{R}^2 = R^2H^2 = \frac{r_{SW}}{R} \tag{48}$$

$$\dot{T} = \frac{1}{1 - R^2H^2} \quad \Rightarrow \quad T = \int \frac{da}{H(a-1)} \tag{49}$$

This results in $2\Psi = 2\Phi = 2\Phi_W = -H^2R^2 = -r_{SW}/R$ in the junction Σ, as in Eq.37. This is the dSE generalization of dS space for arbitrary $a(\tau)$: $2\Psi = 2\Phi = -R^2/r_H^2$ with $r_H \equiv 1/H(\tau)$ in Eq.29. Note how Eq.49 is the generalization of Eq.33 for $\dot{H} \neq 0$ and it agrees with $\partial_\tau t = (1 + 2\Phi_W)^{-1}$ in Eq.30 for $2\Phi_W = -H^2R^2$. The Event Horizon $2\Phi = -1$ corresponds to $R = r_{SW} = r_H$ and the critical density inside r_H corresponds to that of a BH in Eq.1 at any time: $8\pi G\rho/3 = H^2 = r_H^{-2} = r_{SW}^{-2}$. This Σ junction grows and reaches $R = r_{SW} = r_H$ at $a = 1$. It takes $T = \infty$ in the SW time of Eq.49 to asymptotically reach $r_{SW} = r_\Lambda$ (see Fig.3). In this limit, Eq.48 reproduces the BH.fv null junction of Eq.44 for constant $H = H_\Lambda$. Before that, the BHU junction is not static (not even in the SW frame) as H decays into H_Λ when R grows towards r_Λ. Despite the discontinuity in ρ, the BHU metric and extrinsic curvature are continuous when we join them with the expanding timelike hypersurface of Σ. This proofs that the BHU metric is also a solution to EFE and there are no surface terms in the junction.

3.5 Types of BHU and BH mass

Note that the above equations do not assume that r_{SW} is constant as a function of τ or t. Even when r_{SW} is constant as a function of t it could vary as function τ because $\tau = \tau(t, r)$ (e.g. see Eq.33). Indeed, Eq.48 shows that the SW radius can evolve as a function of comoving time τ using $R = a\chi_{SW}$:

$$r_{SW} = \frac{R^3}{r_H^2} = \begin{cases} 2GMa^{-1} & \text{for a radiation dominated BH.r} \\ 2GM & \text{for a matter dominated BH.m} \\ r_\Lambda & \text{for a } \rho_\Lambda \text{ dominated BH.fv} \end{cases} \tag{50}$$

where M is the total (true) matter/radiation energy inside the comoving radius $r_{SW} \equiv 2GM_{SW}$. The junction grows as $R = a\chi_{SW}$ in comoving coordinates (with $a < 1$). It takes infinite time $T = \infty$ in the SW frame to reach $a = 1$ in the comoving frame (see Eq.49). This is illustrated in Fig.4.

We call BH.m (BH.r) a matter (radiation) dominated BH. These are types of BHU or more generally different phases in the BHU evolution. Starting from early times (i.e. small τ or $a << 1$), for the outside observer the BH mass first decreases (during radiation domination BH.r) before it becomes constant (during matter domination BH.m). If there is a FV or $\rho_\Lambda \neq 0$ it grows again to become constant at $r_{SW} = r_\Lambda$. Recall that as we approach $a = 1$ the FLRW event horizon r_* in Eq.18 and Fig.2, evolves from being constant in comoving coordinates to being constant in physical coordinates and in this limit we reproduce the null junction solution in Eq.44. Solutions with $H < 0$ are also allowed by the junction conditions. In this case we would have contraction instead of expansion.

If we (gravitationally) detect a BH.r of mass M at some time $a < 1$ we should find that r_{SW} is larger than $2GM$ (smaller for $H < 0$). This could result in observational evidence for these BHU solutions and the existence a of BH.r type. But because we are used to SW black holes, we might not call this a BH (usually BHs are defined as objects for which $r_{SW} = 2GM$). Note that this is different from a Supernova explosion because radiation is always trapped inside r_{SW} for the outside observer. So no radiation escapes outside r_{SW}.

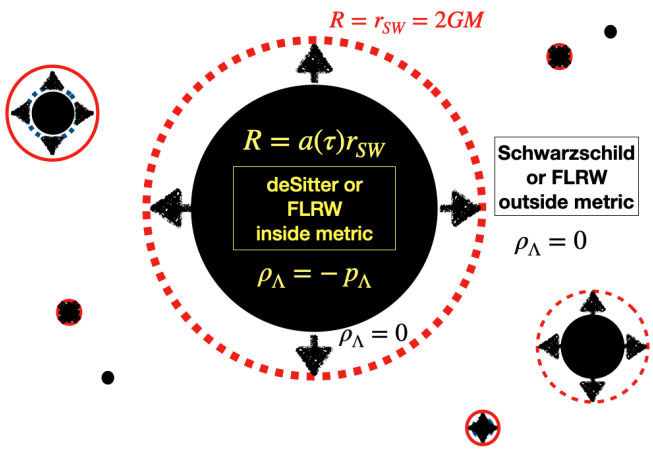

Figure 4. Illustration of the interior dynamics of a BHU. The junction $R = a(\tau) r_\Lambda$ (black disk) grows towards a trapped surface $R = r_\Lambda = r_{SW}$ (dashed red circle). The inside of $R = a(\tau) r_\Lambda$ is FLRW or dS metric while the outside is the empty BH.SW metric, which can also be interpreted as a perturbation around an exterior FLRW background, possibly with other BHs and matter.

If matter or radiation from outside fall inside r_{SW} for a BH.m or BH.r, the internal BH mass (and r_{SW} radius) will increase. This is what we usually assume happens for a BH.SW. So matter is conserved for the inside and outside observer. But if matter falls on a generic BHU which also contains some ρ_Λ, M will first increase but it will eventually be diluted by the internal dS expansion. The final BH mass is always given by $2GM = r_\Lambda = (4\pi\rho_\Lambda/3)^{-1/2}$, which is independent for ρ_m or ρ_R inside. For the inside observer the infall mass lost corresponds to additional expansion energy. But for the external observers this looks like a net mass lost. We conjecture that such mass lost could be compensated by energy ejection from r_{SW} in the form of high energy particles, gamma rays or gravitational waves (assuming the infall is not perfectly symmetrical). This could relate to some direct observational evidence for BHU. In a separate paper (Carcasona & Gaztanaga, in preparation) we elaborate on this point.

3.6 Evolving junction: internal BH dynamics

Our junction solutions are similar to the ones found for Bubble Universes (e.g. see Blau et al. 1987; Aguirre & Johnson 2005 and references therein) but with some important differences. Our case corresponds to the FLRW metric (which could include matter and radiation as well as a FV), which is not static in the SW frame as dS metric. The Bubble Universes only use dS metric. Also, a surface term with $\sigma \neq 0$ is always needed to glue the resulting discontinuities. This happens because they use a different coordinate system and therefore junction condition. The BHU junction $r = R(\tau)$ has no surface terms ($\sigma = 0$) and therefore no bubble. We could say that the BH.fv type of BHU is like a Bubble Universe without bubble.

The junction conditions indicate that the division between interior and exterior solutions in Eq.37 is not r_{SW} or r_Λ, which are only the limiting cases, but R. This is illustrated in Fig.4 (see also Fig.5). That both the metric and the extrinsic curvature are continuous at Σ shows that there are no surface terms and the join metric is a solution to EFE (see Eq.21.167 in Misner et al. 1973). The energy-momentum tensor $T_{\mu\nu}$ corresponding to these solutions has a discontinuity as expected for a BH, but not the metric: there is no bubble.

Inside the physical BH we have an expanding junction: $r = R(\tau)$. Because $R(\tau) < r_{SW}$ the external SW observer can not distinguish this evolving junction from the limiting static one $r = r_{SW}$. This is why we chose to express the solution this way. The junction $R(\tau)$ grows and asymptotically tends to r_{SW} as shown in Fig.4. This happens at a finite comoving time τ_Λ as in the top panel of Fig.3. The exact function depends on the form of $a = a(\tau)$. For constant $H = H_\Lambda = 1/r_{SW}$, the solution can be expressed analytically as:

$$R(\tau) = R_0 e^{H_\Lambda \tau} = e^{H_\Lambda(\tau - \tau_\Lambda)} r_{SW} \tag{51}$$

where we have chosen $a = 1$ when $R = r_{SW}$. We start with a finite size $R = R_0 = a_0 r_{SW}$ at $\tau = 0$, where $a_0 = e^{-\tau_\Lambda H_\Lambda}$. After $\tau_\Lambda H_\Lambda$ e-folds, R_0 grows into $R = r_{SW}$. This inflation stops asymptotically at $\tau = \tau_\Lambda = -r_{SW} \ln a_0$. As illustrated in Fig.1, Hubble damping of kinetic K energy can result into a trapped FV region. We can think of R_0 as such FV region $\rho_\Lambda = \Delta$, which (in empty space) will inflate to size $r_{SW} = 1/H_\Lambda = (8\pi G\Delta/3)^{-1/2}$.

This new solution to EFE is not just an arbitrary matching of two other random solutions. It is a new solution of a new physical configuration given by the energy content in Eq.36. This configuration corresponds exactly to our definition of a generic physical BH. The one we set to find in the introduction and whose horizon separates two regions with different matter-energy content. The same horizon defines the junction of two well known solutions to EFE.

3.7 Implications for our Universe

The BH.fv interior, dS metric, can be transformed into a FLRW metric with constant $H = H_{\Lambda\_}$. This frame duality provides a new interpretation for the BH.fv solution in Eq.35. This is not only a solution for a BH inside a universe. The inside comoving observer, sees this solution as an expanding inflationary universe inside a BH, even when the metric is static in physical SW coordinates and $r = r_{SW}$ is fixed. The same happens with the BH.u solution of Eq.37, which is equivalent to a child FLRW in the interior. Recall how the outside BH.SW solution should be considered a perturbation of a parent FLRW in Eq.22. So we have two nested FLRW metrics which are connected with the BHU. Each one could have a different effective ρ_Λ (or FV). So could our universe be a child FLRW metric? The fact that we have measured $\rho_\Lambda \neq 0$ provides a strong indication that this is the case. It is hard to explain what Λ or the coincidence problem mean otherwise (see e.g. Weinberg 1989; Peebles & Ratra 2003).

The change of variables in Eq.30 is only valid for physical SW coordinates that are centered at the center of the BH location. But in the transformed (comoving) frame of Eq.32 any point inside is subject to the same expansion law with equal $a(\tau)$. From every point inside de BHU, comoving observers will see an homogeneous and isotropic space-time around them (see bottom left of Fig.6). But recall from Fig.2 the the observable universe eventually becomes larger than the FLRW trapped horizon. All points inside the BH were at the center in their distance past (just as in the homogeneous expanding universe). As they look back in time from a position that is off centered, some regions of the sky will observe different parts of what is outside. This could result in some significant deviations from isotropy and homogenety on the largest scales. Regions outside the trapped surface could have a similar background but with uncorrelated fluctuations resulting in fits to different cosmological parameters. Such anomalies have already been measured in the CMB maps (see Fosalba & Gaztañaga 2021; Gaztañaga & Fosalba 2021).

Note how we can have FVs inside other FVs (see Fig.1). So we can have BHs inside other BHs or FLRW metrics inside other FLRW universes. Mathematically this looks like a Matryoshka (or nesting) doll or a fractal structure (see also Fig.4 in Gaztañaga 2021). But physically, in the common SW frame, each BH has a different mass

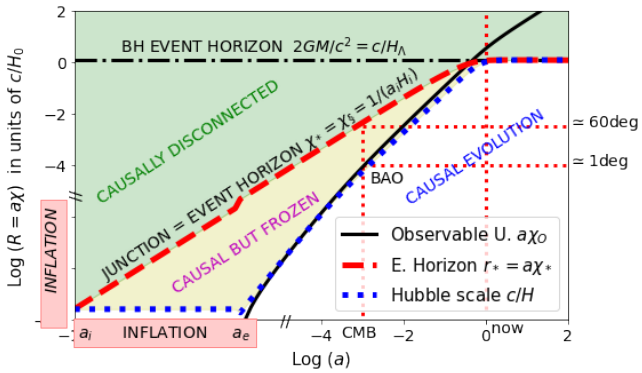

Figure 5. Extension of Fig.2 to the period of inflation. The FLRW Event Horizon $r_* = a\chi_*$ in Eq.18 (red dashed line) here is also the BHU junction and matches the primordial causal boundary for inflation $\chi_* = \chi_\S$. Scales larger than r_* are causally disconnected (green shading). Our event horizon today $a\chi_* \simeq c/H_\Lambda$ becomes the BH event horizon (dot-dashed line) in the SW frame.

and therefore different physical properties. The child FLRW BHU have smaller mass (and larger FV) than the parent BHU. A BHU of one solar mass can have a FLRW metric inside but this inside will not have any galaxies and is going to be very different from that in a $M \simeq 5.8 \times 10^{22} M_\odot$ BHU, like ours, which contains billions of galaxies and BHs of many different sizes. So each BHU layer could be physically quite different from the next, unlike Matryoshka dolls or a fractal structure.

3.8 The evolution of the BH universe

How did the universe evolve into the solution of Eq.37? This is an important question. It is not enough to find a solution to EFE. We need to make sure that such a configuration can be achieved in a causal way. A good example of this is the standard FLRW solution. Without Λ, the FLRW universe has no causal origin: the Hubble rate (in Eq.15) is the same everywhere, not matter how far, and this is not causally possible (Gaztañaga 2020; Gaztañaga 2021). The comoving coordinate $\chi = r_{SW}$ that fixes the junction in §3.4 above can be identified as the causal horizon $\chi_\S$ in the zero action principle (see Eq.7 and Gaztañaga 2021). In the FLRW Universe, the Hubble Horizon r_H is defined as $r_H = c/H$. Scales larger than r_H cannot evolve because the time a perturbation takes to travel that distance is larger than the expansion time. This means that $r > r_H$ scales are "frozen out" (structure can not evolve) and are causally disconnected from the rest (e.g. see Dodelson 2003). Thus, c/H represents a dynamical causal horizon that is evolving. This was illustrated in Fig.2.

A possible evolution of our universe is shown in Fig.5. Note that here we choose $a = 1$ now, as opposed to§3.4 where $a = 1$ corresponds to $R = r_{SW}$. It turns out that both are not so different according to some measures (the so call coincidence problem in cosmology). A primordial field φ settles or fluctuates into a false (or slow rolling) vacuum which will create a BH.fv with a junction Σ in Eq.45, where the causal boundary is fixed in comoving coordinates and we assume it corresponds to the particle horizon during inflation $\chi_\S = c/(a_i H_i)$ or the Hubble horizon when inflation begins. The size $R = a(\tau)\chi_\S$ of this vacuum grows and asymptotically tends to $r_H = c/H$ following Eq.48 with $H = H_i$. The inside of this BH will be expanding exponentially $a = e^{\tau H_i}$ while the Hubble horizon is fixed $1/H_i$. Accooring to standard models of primordial inflation (Starobinskiĭ 1979; Guth 1981; Linde 1982; Albrecht & Steinhardt 1982), this inflation ends (at some a_e) and vacuum energy excess converts into matter and radiation (reheating). This results in BH.u, where the infinitesimal Hubble horizon starts to grow following the standard BB evolution.

Note that the inflation in the BH.fv solution (i.e. Eq.51) stops naturally at cosmic time $\tau_i = -H_i^{-1} \ln \chi_\S H_i$ (see Fig.3) when physical SW distance is $r = a(\tau)\chi_\S = 1/H_i$. In standard models of primordial inflation, H_i is much larger that H_Λ so that $1/H_i$ is much smaller than $1/H_\Lambda$. So a FV Δ only grows to a maximun size $R = r_{SW} = (8\pi G\Delta/2)^{-1/2} = 1/H_i$. Something else has to happen if we want the size to become cosmological. It could be reheating or some other mechanism. Quantum tunneling into smaller Δ (see Fig.1) also produces larger r_{SW}. Matter and radiation can also appear some other ways: from the original quantum fluctuations, from quantum tunneling to/from other FV, from infall of matter from outside (see §2.1-4.3) or from Hubble damping of smaller FV that turn into BHs (see §2.1). Regardless of these formation details, $\chi_\S$ remains the causal scale for the original BH.fv inflation in Eq.51. Recall that the BH.fv solution requires a discontinuity in $\rho_\Lambda = 0$, so this BH.fv evolution happens with independence of what we assume about Λ in EFE. A causal boundary in empty space generates a boundary term in the action that fixes the value of Λ to $\Lambda = 4\pi G < \rho + 3p >$, where the average is over the light-cone inside $\chi_\S$ (see Eq.7 and Gaztañaga 2021). This effective Λ represents a trapped surface for the emerging BHU.

The comoving observable universe after inflation (see also Eq.19) is:

$$\chi_O = \chi_O(a) = \int_{a_e}^{a} \frac{d \ln a}{aH(a)} = \chi_O(1) - \bar{\chi}(a), \tag{52}$$

For $\Omega_\Lambda \simeq 0.7$, the particle horizon today is $\chi_O(1) \simeq 3.26 c/H_0$ and $\bar{\chi}(a) = \int_a^1 d \ln a/(aH)$ is the radial lookback time, which for a flat universe agrees with the comoving angular diameter distance, $d_A = \bar{\chi}$. The observable universe $a\chi_O$ becomes larger than $r_{SW} = r_\Lambda$ when $a > 1$ as shown in Fig.5 (see also Fig.2). This shows that, observers like us, living in the interior of the BHU, are trapped inside $r_* = a\chi_*$ but can nevertheless observe what happened outside. We can estimate $\chi_\S$ from $\rho_\Lambda =< \rho_m/2 + \rho_R >$, where the average is in the lightcone inside $\chi_\S$. For $\Omega_\Lambda \simeq 0.7$, Gaztañaga (2021) found: $\chi_\S \simeq 3.34 c/H_0$ which is close to χ_O today. It is natural to interpret the observed Ω_Λ as a causal boundary because it does generate an event horizon χ_* in Eq.18. But let us assume that Ω_Λ (or χ_*) have nothing to do with the causal horizon $\chi_\S$ from inflation. This was illustrated in Fig.2, which shows two different causal regions. If we identified $\chi_\S$ (instead of $\chi_* < \chi_\S$) with the BHU junction, we would still have that $\chi_\S \lesssim \chi_O$, because otherwise $\chi_\S$ would have met $RH = 1$ early on, resulting in smaller χ_O than measured (compare Fig.2 to Fig.5).

Thus, at the time of CMB last scattering (when $d_A \simeq \chi_O$), $\chi_\S$ corresponds to an angle $\theta = \chi_\S/d_A \lesssim 1$ rad $\simeq 60$ deg. So we can actually observe scales larger than $\chi_\S$. Scales that are not causally connected! This could be related to the so-called CMB anomalies (i.e, apparent deviations with respect to simple predictions from ΛCDM, see Gaztañaga 2021; Fosalba & Gaztañaga 2021; Gaztañaga & Fosalba 2021 and references therein), or the apparent tensions in measurements from vastly different cosmic scales or times (e.g. Planck Collaboration 2020; Riess 2019; DES Collaboration 2019; Di Valentino et al. 2021).

4 DISCUSION & CONCLUSION

Table 1 shows a summary of notation and metrics considered in this paper. The SW metric in Eq.26 is well known and studied but the interior solution is not physical because it corresponds to a singular point source. Moreover a BH interior can not be made out of regular matter because according to GR an object of mass M must have a minimal radius given by Eq.2 (Buchdahl 1959). What is inside a BH then? We have looked for classical non-singular GR solutions for a BH interior. Our motivation is to find a physical model and study if this results in some different observed properties for BHs. The outside manyfold $\mathcal{M}_+$ of a BH is approximated as empty space so the solution g_+ is the BH.SW metric. Because the inside $\mathcal{M}_-$ is causally disconnected, $\mathcal{M}_+$ acts like a simple boundary condition. Given some ρ and p inside r_{SW}, we have solve EFE inside with such boundary condition to find g_-, the inside metric of a physical BH. To our surprise we have found that g_- is just the well known FLRW, the same metric that describes our universe! This frame duality, represented by Eq.30, has several observational consequences, as we will discuss below.

To impose the boundary at r_{SW} we have use the same (physical) outside SW frame that is not moving with the inside perfect fluid, so that $T^1_0 \neq 0$. This results in a solution for $\mathcal{M}_-$ that is not static, which explains how we can avoid the constrain in Eq.2. We have verified Israel´s conditions to double check that the join manyfold $\mathcal{M}_- \cup \mathcal{M}_+$ is also a solution to EFE and there are no surface terms (see §3.4). This is different from just matching two arbitrary metrics because they correspond to well defined energy content configuration in Eq.36. We can add matter and radiation to both sides of r_{SW} and we still have a BHU solution. The BHU connects two FLRW metrics (see Fig.6) joined by a BH event horizon, which corresponds to a FLRW event horizon in Eq.18.

The relativistic Poisson equation comes from the geodesic deviation (see Eq.12 in Gaztañaga 2021):

$$\begin{aligned} \nabla_\mu \mathsf{g}^\mu &= \frac{d\Theta}{ds} + \frac{1}{3}\Theta^2 = R_{\mu\nu}u^\mu u^\nu \\ &= \Lambda - 4\pi G(\rho + 3p) = 8\pi G\left[\rho_\Lambda - \rho_m/2 - \rho_R\right] \end{aligned} \quad (53)$$

where g^μ is the geodesic acceleration (Padmanabhan 2010). This is also the Raychaudhuri equation for a shear free, non rotating fluid where $\Theta = \nabla_\nu u^\nu$ and s is proper time. The above equation is purely geometric: it describes the evolution in proper time of the dilatation coefficient Θ of a bundle of nearby geodesics. Note how only $\rho_\Lambda > 0$ produces the observed acceleration (and therefore expansion).

A key point to the BHU solution is the discontinuity at $r = r_{SW}$ which could also be understood as a boundary to the Einstein-Hilbert action, see Eq.7. Because the BHU is trapped inside $\chi_\S$ we might expect $S^{on-sh} = 0$. Using Eq.53 in Eq.7:

$$\rho_{\Lambda_-} = < \rho_m/2 + \rho_R >_{\chi_\S}, \quad (54)$$

where the average is inside the lightcone to $\chi_\S$. This can be used to estimate $\chi_\S$ (Gaztañaga 2021) and sheds new light over the measured coincidence between ρ_{Λ_-} and ρ_m. But note that if the outside of the BHU is not empty, the inside is not really a closed or isolated system as matter and radiation can fall inside. In Appendix C we consider such more general case.

4.1 False Vaccum BH solution (BH.fv)

BH.fv corresponds to constant FV discontinuity (Eq.34) with dS metric inside (Eq.35), with a trapped surface which matches the BH.SW event horizon. A constant density (or negative pressure) corresponds to a centrifugal force, $2\Phi = -(r/r_{SW})^2$ that opposes Newtonian gravity, $2\Phi = -r_{SW}/r$, i.e. Eq.24. The equilibrium happens when both forces are equal, which fixes $r = r_{SW}$, and is the equivalent of the stable circular Kepler orbits in Newtonian dynamics.

This solution is similar to the classical Bubble Universe solution (Blau et al. 1987; Frolov et al. 1989; Aguirre & Johnson 2005; Garriga et al. 2016; Kusenko 2020) including the gravastar (Mazur & Mottola 2015) and other extensions (e.g. Easson & Brandenberger 2001; Daghigh et al. 2000; Firouzjahi 2016; Oshita & Yokoyama 2018; Dymnikova 2019). But there are some important differences. In §3.4 we show that there are no surface terms. We find that a nullike hypersurface Σ , in Eq.44, provides a continuous solution. The same solution is also found in the asymptotic limit ($a = 1$) for a timelike hypersurface Σ of Eq.48.

So contraty to Bubble Universes, there is no bubble in BH.fv. As far as we know, this is new and different from anisotropic models with negative radial pressure (Brustein & Medved 2019; Dymnikova 2019) or the above Bubble Universes, which have $\sigma \neq 0$ over a spacelike or null bubble hypersurface. Moreover, a fix comoving scale has a physical meaning. It corresponds to a causal horizon $\chi_\S$, given by the particle or Hubble horizon for an expanding background, such as cosmic inflation or a rapid supernova explosion.

4.2 The BH universe solution (BH.u)

In Eq.37 the BH interior is the FLRW metric. This BH.u solution is new, as far as we know. As discuss in the introduction, previous proposals were not proper or complete solutions within classical GR. We can have other BHs, matter and radiation inside a BHU. The inside needs to be expanding as in the FLRW metric of Eq.12, with a trapped surface given by ρ_Λ. This holds the expansion and balance gravity at r_{SW} as in the BH.fv solution. The join FLRW+SW solution (Eq.37) is also a solution to Einstein's field equations as the two metrics reduce to the same form on a junction of constant $\chi = r_{SW}$ in Eq.45, and the extrinsic curvature in Eq.47 is the same in both sides. The junction $R(\tau)$ between interior and exterior solutions in Eq.35 and Eq.37 is not necessarily $R = r_\Lambda = r_{SW}$, which is just the limiting case. The junction $R(\tau)$ asymptotically tends to r_{SW} as illustrated by Fig.4.

In section §3.5 we define 2 new types of possible BH interiors corresponding to matter (BH.m) or radiation (BH.r) dominated BH. As far as we know these are new classical BH solutions to GR. Stuckey (1994) presented a solution which is similar to BH.m (but with a null junction instead of a timelike junction), as a possible cosmological model without Λ or radiation.

As happens for the SW metric, the exterior metric of the BHU could also be FLRW. The outside space is approximated as empty space, but more realistically is a local perturbation within a larger FLRW background (e.g. see Eq.22 and Kaloper et al. 2010). This is illustrated in bottom right of Fig.6. In this case we need to distinguish between two different effective ρ_Λ, the one in the inside FLRW metric, ρ_{Λ_-} and the one for the outside, ρ_{Λ_+}, which should be smaller (see Appendix B-C).

The solutions to the field equations are independent of the choice of coordinates but $\bar{T}_{\mu\nu}(t, r)$ depends on the fluid motion (see Eq.38) which indicates that the BH interior is not static, as usually assume (Buchdahl 1959). We used comoving coordinates (τ, χ), where the fluid is expanding and the observed is comoving, to find the interior solution. But we can then transform back to physical SW frame (t, r), using the duality transformation Eq.30, to find a full BH solution in Eq.37 that is continuous in the metric and curvature at r_{SW}, like in the BH.fv case. As it happens with the SW metric, outgoing radial

null geodesics cannot escape the event horizon, but incoming ones can enter (see discussion around Eq.18). So the BHU solution is a physical BH.

4.3 BH formation

Another issue, which we only address partially in §2.1, is how such physical BHU solutions can be achieved (e.g. astrophysical and primordial BH formation) and if they can have a causal origin. There is extensive literature on Bubble Universe formation (e.g. see Garriga et al. 2016; Oshita & Yokoyama 2018 and references therein) but they typically involve quantum gravity ideas or GR extensions. As discussed in §2.1, Hubble damping of the kinetic energy K of a classical scalar field φ (see Fig.1) can result in a FV trapped field configuration. Such initially small local discontinuity, with FV energy density Δ, will grow as Eq.51 until it reaches the stable BH size corresponding to $\rho_{BH} = \Delta$. So Δ is the BH.fv density: the smaller Δ the larger the BH size and mass. As illustrated in Fig.1 if we think of $V(\varphi)$ as the superposition of many plane waves of different frequencies this will result in a landscape of nested BHU of different masses and sizes. Note how the masses and sizes of such BH.fv bares no relation with the energy of the expansion (e.g. supernova explosion) which originates it.

Could a BHU formed just from the final collapse of a dying star? In the latest stages of a stellar collapse there has to be some bouncing that avoids the singularity resulting in a supernova explosion. The matter and radiation that is trapped inside the SW radius will be expanding in a FLRW metric and will correspond to a BHU of type BH.m, BH.r or a mix. Any field present will suffer Hubbble damping and may end up in a FV. In such case the final BHU could also end as a BH.fv. As argued below Eq.50 the true mass of such BH could be different from $M_{SW} \equiv r_{SW}/2G$ and matter and radiation falling inside might not just increase the final SW radius as it is usually assumed.

These ideas are speculative but plausible. The point we want to make here is that the BH interior is important for models of BH formation and abundance (e.g. BHs as DM candidates). Such interior can be made of non singular classical BHU rather than a singular SW.BH or some Quantum Gravity equivalent. Further work is needed to understand such BHU formation and evolution.

4.4 What is M for a physical BH?

For a stellar or galactic BH within a larger universe (where we neglect Λ_+ or V_0 outside), the BH mass M in the BHU is asymptotically given by the FV excess energy Δ, so that ρ_{BH} in Eq.1 is $\rho_{BH} = \Delta$ and $M = (32\pi G^3\Delta/3)^{-1/2}$. For a more general case see Eq.B3. So the larger Δ the smaller the BH mass and size. This is independent of the matter and energy content that falls inside the BH. So M in the BHU solution does not correspond to the actual total mass or radiation inside, which is not observable from the outside, but should instead be interpreted in terms of the FV energy excess Δ. This could have implications for models of astrophysical BH formation (e.g. Kormendy & Ho 2013 and references therein) and primordial BH formation (e.g. Kusenko 2020 and references therein) which usually assume that BH accretion and merging results in linear increase of the BH mass M.

The BHU is static from the point of view of the outside SW frame. The BH.u solution in Eq.37 is achieved in the limit where the interior dynamics is dominated by $\rho_\Lambda = \Delta$. But the BH.u solution is also valid for a junction $R = 1/H < r_{SW}$ where the inside dynamics is not yet dominated by Δ. These BHs are expanding also in the SW frame, but this expansion happens inside r_Λ (see Fig.4). In the limit in which Δ (or ρ_Λ inside) can be neglected and the BH is of type BH.m or BH.r, the BH mass is given by Eq,50. The external observer can not differentiate this form a static BH. This is why we prefer to show the solution as in Eq.37 in terms of r_{SW}. Mass accretion only adds to ρ_m which will change the internal FLRW dynamics (and will be "burnt" or diluted away), but will not change the BH mass, Δ or r_{SW}.

4.5 Our universe as a BH

The BHU can be interpreted as a BH within our universe or as an expanding universe inside a larger space-time. As pointed out in the introduction, that the universe might be generated from the inside of a BH has a long and interesting history. Knutsen (2009) argued that p and ρ in the homogeneous FLRW solution are only a function of time (in comoving coordinates) and can not change at $r = r_{SW}$ to become zero in the exterior. This argument seems to contradict the BHU solution. The riddle is resolved with ρ_Λ. Without ρ_Λ the FLRW universe can not have a causal origin: the comoving density and Hubble rate are the same everywhere, and this is not causally possible (Gaztañaga 2020; Gaztañaga 2021). A causal horizon $\chi_\S$ fixes ρ_Λ (see Eq.54) which solves this problem and also generates an even horizon $\chi_\S = \chi_*$ (see Eq.18) similar to that of a SW metric. This allows for an homogeneous FLRW solution inside r_{SW} but with a discontinuity at r_{SW}, so that it is in-homogeneous in the join manyfold $\mathcal{M} = \mathcal{M}_- \cup \mathcal{M}_+$ of the physical SW frame.

Homogeneity is therefore the illusion of the comoving observer inside r_{SW}. The FLRW metric is trapped inside r_* (Eq.18), and is then equivalent to an inhomogeneous spherically symmetric metric of Eq.32. The FLRW metric is only homogeneous in space, but not in space-time. A new frame where comoving time and space are mixed, can break or restore this symmetry. The frame duality in Eq.30 is only valid for physical coordinates that are centered at the BH location. But in the transformed (comoving) frame any point inside the BHU is subject to the same expansion law with equal $a(\tau)$. From every point inside de BHU, observers will see an homogeneous and isotropic space-time around them. Just like in the universe around us.

4.6 Evidence for a BHU

We can sketch the evolution of our universe with this BHU model (see Fig.4-5). In physical coordinates this solution has no BB (or bounce): it is not singular at $r = 0$ or $t = 0$, because we have a non-singular BH.fv start before the FLRW BH.u phase. The inside comoving observer is trapped inside $r < r_{SW}$ and has the illusion of a BB. The space-time outside (the parent FLRW universe) could be longer and larger than the BB comoving observer estimates. We could have a network of island universes with matter and radiation in between. To some extend this is also the case for some models of inflation within the standard BB model.

These ideas explain why our universe (or other island universes) is expanding and not contracting. The initial fluctuation that originate our BHU, $H_i^2 = 8\pi G\Delta/3$, could be expanding ($H_i > 0$) or contracting ($H_i < 0$). In the later case it will either recollapse (and disappear) very quickly or it will bounce into expansion dominated by the repulsive gravitational force that results from the negative pressure from constant Δ or Λ (see Eq.53).

We have other observational evidence that the expanding metric around us is inside a BHU. We can recover the BB homogeneous solution in the limit $\Delta \Rightarrow 0$, where we have $r_{SW} \Rightarrow \infty$ and $\rho_\Lambda = 0$.

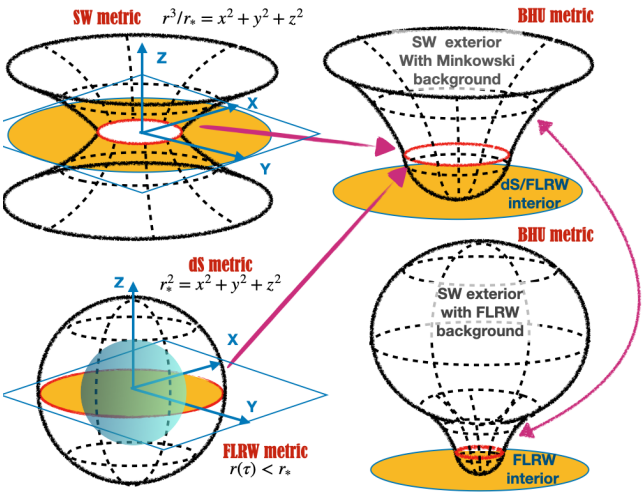

Figure 6. Spatial representation of $ds^2 = (1+2\Phi)^{-1}dr^2 + r^2 d\theta^2$ 2D metric embedded in 3D flat space for: deSitter (dS, bottom left, $2\Phi = -r^2/r_*^2$), FLRW ($r(\tau) < r_*$, blue sphere inside dS), Schwarzschild (SW, top left, $2\Phi = -r_*/r$) and two versions of the combined BHU metrics. Yellow region shows the projection coverage in the (x, y) plane. In the top right figure we show a BHU with dS (or FLRW) interior and SW metric exterior joint at the Event Horizon $r_* = 2GM = 1/H_\Lambda$ (red circles). The BHU solution has in general two nested FLRW metrics join by SW metric (bottom right). See Appendix A for a more detailed explanation.

But we have measured $\rho_\Lambda > 0$ ($\Omega_\Lambda \simeq 0.7$) which implies $M \simeq 5.8 \times 10^{22} M_\odot$ and $r_{SW} \simeq c/H_0$, as in the BHU. The causal interpretation for $\chi_\S$ and the time duality also helps understanding the observed coincidence between ρ_Λ and ρ_m today (Gaztañaga 2020; Gaztañaga 2021). See also Appendix C about the coincidence problem and the causal boundary.

If we look back to the CMB times, $\chi_\S$ corresponds to $\simeq$ 60 degrees in the sky. The observed anomalies in the CMB temperature maps at larger scales (Gaztañaga 2020; Gaztañaga 2021; Fosalba & Gaztañaga 2021; Gaztañaga & Fosalba 2021; Camacho & Gaztañaga 2021) provide additional support to the idea that there is a causal horizon in quantitative agreement with the BHU model. There a window to see outside our BHU using the largest angular scales for $z > 2$ and measurements of cosmological parameters from very different cosmic times. There seems to be already mounting evidence for this (e.g. Planck Collaboration 2020; Riess 2019; DES Collaboration 2019; Di Valentino et al. 2021).

What could falsify the BHU model? For our universe as a BHU a measurement of the DE equation of state $\omega \equiv p/\rho \neq -1$ would indicate that cosmic acceleration is not caused by the causal event horizon r_Λ. For a BHU model as a BH inside our universe, we expect $r_{SW} \neq 2GM$, as such relation only holds asymptotically, see Eq.50. So a direct and precise measurement of both the BH size r_{SW} and its gravitational mass M can be used to rule out the BHU model. Also we would not expect the BH mass to add linearly when matter (or other BHs) fall inside or merge into a BHU. Instead the BHU model predicts that the total mass added to a BHU should decrease as a function of time. This can be verified or falsified with available direct observations (e.g. Carcasona & Gaztanaga, in preparation) and could play some role in understanding the second law for BH thermodynamic analogy (Wald 2001; Dougherty & Callender 2016 and references therein).

If there are other island universes outside ours, Galaxies and QSO, as well as BHs, could have accreted from outside r_Λ into our BHU. Because the horizon $1/H_\Lambda$ is so large, we can only see evidence of those mergers as LSS at early times, during or right after the CMB, when $\chi_\S$ subtends $\simeq$ 60deg. on the sky and the universe becomes transparent. Possible relics around us should have been erased during radiation domination. But some relics could have entered after matter domination, in or distant past. If we measured the age of an object (e.g. star, QSO or galaxy) which is older than the BB this will be a clear indication in favour of the BHU model. If our universe merged with another BHU which was few % smaller, we might be able to see such % glitches in $H(z)$ with current or future data.

Another possible observational evidence for the BHU solution is outgoing high energy cosmic rays or GW background signal from BH accretion or mergers within our BHU (see §3.5). High energy cosmic rays have been linked with X-ray binaries and AGNs, both hosting BH of different masses. Such GW background signal could also be observable as CMB tensor fluctuations.

There is good observational evidence for homogeneity and lack of correlations in the CMB at $r > r_\Lambda$ (see Camacho & Gaztañaga 2021 and references therein). This suggests that the underlying physical mechanism sourcing the observed anisotropy encompasses scales beyond our causal universe. This agrees with the variations found in cosmological parameters over large CMB regions (Fosalba & Gaztañaga 2021), which is the largest reported evidence for a violation of the Cosmological principle. Such observations indicate a breakdown of the standard BB picture in favor of the BHU. Fig.31 in Fosalba & Gaztañaga (2021) shows that the size of these causal regions follow the BHU relation between $\chi_\S$ and ρ_Λ. This is consistent with the idea that the causal scale of inflation is responsible for the observed ρ_Λ (compare Fig.2 to Fig.5) and that our universe was accreted into or created by a larger BHU. The BHU model allows for a Perfect Cosmologocal Principle, the one advocated by Einstein (when he introduced Λ) and the Steady State Cosmology (O'Raifeartaigh & Mitton 2015; Bondi & Gold 1948; Hoyle 1948). But there is no need for ad hoc matter creation to explain the observed cosmic expansion. The frame duality allow us to understand how we can have at the same time an expanding universe in comoving coordinates (as observed by the Hubble-Lemaitre law) and a static BHU in the outside SW frame.

ACKNOWLEDGMENTS

I want to thank Marco Bruni, Robert Caldwell, Ramin G. Daghigh, Alberto Diez-Tejedor and Angela Olinto, for their feedback. This work has been supported by spanish MINECO grants PGC2018-102021-B-100 and EU grants LACEGAL 734374 and EWC 776247 with ERDF funds. IEEC is funded by the CERCA program of the Generalitat de Catalunya.

DATA AVAILABILITY STATEMENT

No new data is presented in this paper.

References

Aguirre A., Johnson M. C., 2005, PRD, 72, 103525
Albrecht A., Steinhardt P. J., 1982, PRL, 48, 1220
Blau S. K., Guendelman E. I., Guth A. H., 1987, PRD, 35, 1747
Bondi H., Gold T., 1948, MNRAS, 108, 252
Brustein R., Medved A. J. M., 2019, PRD, 99, 064019
Buchdahl H. A., 1959, Phys. Rev., 116, 1027

Camacho B., Gaztañaga E., 2021, arXiv e-prints, p. arXiv:2106.14303
DES Collaboration 2019, PRL, 122, 171301
Dadhich N., 2007, Pramana, 69, 23
Daghigh R. G., Kapusta J. I., Hosotani Y., 2000, arXiv:gr-qc/0008006,
Deser S., Franklin J., 2005, American Journal of Physics, 73, 261
Di Valentino E., et al., 2021, Classical and Quantum Gravity, 38, 153001
Diez-Tejedor A., Feinstein A., 2006, PRD, 74, 023530
Dodelson S., 2003, Modern cosmology, Academic Press, NY
Dougherty J., Callender C., 2016, Black Hole Thermodynamics: More Than an Analogy?, http://philsci-archive.pitt.edu/13195/
Dymnikova I., 2003, International Journal of Modern Physics D, 12, 1015
Dymnikova I., 2019, Universe, 5, 111
Dyson L., Kleban M., Susskind L., 2002, J.of High Energy Phy, 2002, 011
Easson D. A., Brandenberger R. H., 2001, J. of High Energy Phy., 2001, 024
Einstein A., 1916, Annalen der Physik, 354, 769
Ellis G., 2008, Astronomy and Geophysics, 49, 2.33
Ellis G. F. R., Rothman T., 1993, American Journal of Physics, 61, 883
Ellis G., Silk J., 2014, Nature, 516, 321
Firouzjahi H., 2016, arXiv e-prints, p. arXiv:1610.03767
Fosalba P., Gaztañaga E., 2021, MNRAS, 504, 5840
Frolov V. P., Markov M. A., Mukhanov V. F., 1989, Phys Let B, 216, 272
Galtsov D. V., Lemos J. P., 2001, Classical and Quantum Gravity, 18, 1715
Garriga J., Vilenkin A., Zhang J., 2016, JCAP, 2016, 064
Gaztañaga E., 2020, MNRAS, 494, 2766
Gaztañaga E., 2021, MNRAS, 502, 436
Gaztañaga E., Fosalba P., 2021, p. arXiv:2104.00521
Good I. J., 1972, Physics Today, 25, 15
Guth A. H., 1981, PRD, 23, 347
Hilbert D., 1915, Konigl. Gesell. d. Wiss. Göttingen, Math-Phys K, 3, 395
Hoyle F., 1948, MNRAS, 108, 372
Israel W., 1967, Nuovo Cimento B Serie, 48, 463
Kaloper N., Kleban M., Martin D., 2010, PRD, 81, 104044
Knutsen H., 2009, Gravitation and Cosmology, 15, 273
Kormendy J., Ho L. C., 2013, ARAA, 51, 511
Kusenko A. e., 2020, PRL, 125, 181304
Lanczos K., 1922, Phys.Z., 23, 539
Lanczos K., Hoenselaers C., 1997, GR and Gravitation, 29, 361
Landsberg P. T., 1984, Annalen der Physik, 496, 88
Linde A. D., 1982, Physics Letters B, 108, 389
Mazur P. O., Mottola E., 2001, arXiv e-prints, pp gr–qc/0109035
Mazur P. O., Mottola E., 2015, Classical and Quantum Gravity, 32, 215024
Misner C. W., Thorne K. S., Wheeler J. A., 1973, Gravitation
Mitra A., 2012, Nature Sci. Reports, 2, 923
O'Raifeartaigh C., Mitton S., 2015, p. arXiv:1506.01651
Oshita N., Yokoyama J., 2018, Physics Letters B, 785, 197
Padmanabhan T., 2010, Gravitation, Cambridge Univ. Press
Pathria R. K., 1972, Nature, 240, 298
Peebles P. J., Ratra B., 2003, Reviews of Modern Physics, 75, 559
Penrose R., 2006, Conf. Proc. C, 060626, 2759
Planck Collaboration 2020, A&A, 641, A6
Popławski N., 2016, ApJ, 832, 96
Riess A. G., 2019, Nature Reviews Physics, 2, 10
Smolin L., 1992, Classical and Quantum Gravity, 9, 173
Starobinskiĭ A. A., 1979, Soviet J. of Exp. and Th. Physics Letters, 30, 682
Stuckey W. M., 1994, American Journal of Physics, 62, 788
Wald R. M., 2001, Living Reviews in Relativity, 4, 6
Weinberg S., 1972, Gravitation and Cosmology, John Wiley & Sons, NY
Weinberg S., 1989, Reviews of Modern Physics, 61, 1
Weinberg S., 2008, Cosmology, Oxford University Press
Zhang T. X., 2018, Journal of Modern Physics, 9, 1838

APPENDIX A: GEOMETRICAL REPRESENTATIONS

To visualize the BHU metric in a 2D plot we consider the most general shape for a spherically symmetric metric in 2D space (x, y) embedded in 3D flat space (x, y, z). In polar coordinates (r, θ) with $r^2 = x^2 + y^2$ and $\tan\theta = x/y$ we have:

$$ds^2 = \frac{dr^2}{1+2\Phi} + r^2 d\theta^2 \tag{A1}$$

In 3D space we just have one additional angle, δ, in Eq.20, but the radial part is the same. The case $\Phi = 0$ corresponds to flat space: $ds^2 = dx^2 + dy^2$. The simplest case with curvature can be represented by a 2D sphere (S2) embedded in 3D flat space using an extra dimension z:

$$ds^2 = dx^2 + dy^2 + dz^2 \quad ; \quad x^2 + y^2 + z^2 = r_*^2 \tag{A2}$$

This metric is flat in 3D coordinates, but constraint to r_*, which is the radius of the sphere and the curvature within the 2D surface of S2. We can replace z by r using: $z^2 = r_*^2 - r^2$ to find:

$$ds^2 = dx^2 + dy^2 + dz^2 = \frac{dr^2}{1 - r^2/r_*^2} + r^2 d\theta^2 \tag{A3}$$

so that $2\Phi = -r^2/r_*^2$ just like in the dS metric of Eq.27 for $r_* = r_\Lambda$. It tell us that dS space corresponds to being in the flat surface of a sphere (like us in Earth). This is illustrated in the bottom left of Fig.6. Note how (r, θ) are coordinates in the (x, y) plane. The S2 space is trapped or bounded by $r < r_*$ (yellow region). The metric changes signature (becomes imaginary) for $r > r_*$: this region can't be reached (white region). The case $r = r_*$ (red circles) corresponds to the Event Horizon at $2\Phi = -1$.

The Newtonian interpretation of $2\Phi = -r^2/r_*^2$ is that this is caused by a centrifugal force, like that in the orbit of a satellite. Even when there is no matter, the curvature (or boundary) is interpret as a repulsive gravitational force that causes acceleration.

The FLRW metric (or dSE metric in Eq.32) correspond to a smaller sphere S2 (inside dS sphere) with an expanding radius $r_H(\tau)$ that tends asymptotically to $r_\Lambda = 1/H_\Lambda$ (see Eq.32):

$$ds^2 = dx^2 + dy^2 + dz^2 \quad ; \quad x^2 + y^2 + z^2 = r_H^2(\tau) \tag{A4}$$

So it has the same topology and Event Horizon or trapped surface (red circle) as dS metric. It is represented in Fig.6 by a blue sphere inside dS sphere in the bottom left corner. This illustrates how it is possible that each observer inside sees an homogeneous space even when the sphere is centered around a given position.

The next simplest case can be represent by a static radius that increases with r:

$$ds^2 = dx^2 + dy^2 + dz^2 \quad ; \quad x^2 + y^2 + z^2 = r^3/r_* \tag{A5}$$

As before, we can replace z by r using: $z^2 = r^3/r_* - r^2$ to find:

$$ds^2 = dx^2 + dy^2 + dz^2 = \frac{dr^2}{1 - r_*/r} + r^2 d\theta^2 \tag{A6}$$

so that $2\Phi = -r_*/r$ just like in the SW metric of Eq.26 for $r_* = 2GM$. This is illustrated in the top left of Fig.6. The case $r = r_*$ (red circle) corresponds to the Event Horizon at $2\Phi = -1$. The Newtonian interpretation for $2\Phi = -r_*/r$ is the inverse square law for a point mass M: $r_* = 2GM$.

The SW space is bounded by $r > r_*$ (yellow region). The metric changes signature (becomes imaginary) for $r < r_*$ and this region can not be reached. This coverage is complementary to dS or FLRW metric which only cover the inner region. We can match the dS and SW metrics at $r = r_*$ to cover the full (x, y) plane as in the BHU metric. Physically this corresponds to a balance between the centrifugal force, represented by dS potential $2\Phi = -r^2/r_*$, and the SW inverse square law, $2\Phi = -r_*/r$, like what happens in the

circular Keplerian orbits.[2] This matching is the junction in Eq.48 which corresponds to a causal boundary. This can also be seem as a Lorentz contraction $\gamma = 1/\sqrt{1-u^2}$ where the velocity u is given by the Hubble-Lemaitre law: $u = Hr$. The time duality between the FLRW and SW frame can also be interpreted as a time dilation, see Eq.32.

This BHU metric is shown in the top right of Fig.6, which is asymptotically Minkowski. The dS metric is the limiting case of FLRW metric and SW metric is a perturbation over FLRW metric. So more generally, the BHU is a combination of 2 FLRW metrics join by a SW metric. The junction happens at the effective value of $r_* = r_\Lambda = 2GM$ corresponding to the inner FLRW ρ_Λ (which we denote as ρ_{Λ_-}). If the outer FLRW has $\rho_{\Lambda_+} \neq 0$, then the SW hyperbolic surface will close as another S2 sphere (bottom right).

APPENDIX B: NON EMPTY SOLUTION

Eq.34 for $V_0 \neq 0$ and $\Lambda \neq 0$:

$$\rho(r) = \begin{cases} V_0 & \text{for } r > r_{SW} \\ V_0 + \Delta & \text{for } r < r_{SW} \end{cases} \tag{B1}$$

can be solved as $\Phi = \Psi$ with

$$2\Phi = \begin{cases} -r_{SW}/r - r^2 H^2_{\Lambda_+} & \text{for } r > r_{SW} \equiv 2GM(1+\epsilon) \\ -r^2 H^2_{\Lambda_-} & \text{for } r < r_{SW} = r_{\Lambda_-} \equiv 1/H_{\Lambda_-} \end{cases} \tag{B2}$$

where $\epsilon \equiv \rho_{\Lambda_+}/\Delta$ and

$$3H^2_{\Lambda_+} \equiv 8\pi G \rho_{\Lambda_+} \quad ; \quad \rho_{\Lambda_+} = \Lambda/8\pi G + V_0 \tag{B3}$$

$$3H^2_{\Lambda_-} \equiv 8\pi G \rho_{\Lambda_-} \quad ; \quad \rho_{\Lambda_-} = \rho_{\Lambda_+} + \Delta \tag{B4}$$

So there are different effective ρ_Λ outside (ρ_{Λ_+}) and inside (ρ_{Λ_-}). The exterior of the BH has the dSW metric but more generally it is a perturbation of the FLRW metric.

APPENDIX C: THE COINCIDENCE PROBLEM

Consider our Universe as the interior of a BHU. For a universe of finite age, there is finite causal boundary M. This requires a boundary term for the action that fixes $\Lambda = 4\pi G < \rho + 3p >$, where the average is over the light-cone inside M (see Eq.7,54). If the causal boundary is set to include $\mathsf{M} = \mathsf{M}_- \cup \mathsf{M}_+$, where M_- and M_+ are the subvolumes inside and outside the BHU, we find:

$$\frac{\Lambda}{4\pi G} =< \rho + 3p >= -2V_0 - 2\Delta \frac{\mathsf{M}_-}{\mathsf{M}} + < \rho_m + 2\rho_R > \tag{C1}$$

We then have that $\rho_{\Lambda_-} = V_0 + \Delta + \Lambda/8\pi G$ becomes:

$$\rho_{\Lambda_-} = \begin{cases} \Delta & \text{for } \mathsf{M}_+ \gg \mathsf{M}_- \\ < \rho_m/2 + \rho_R > & \text{for } \mathsf{M}_- \gg \mathsf{M}_+ \end{cases} \tag{C2}$$

The first case corresponds to a small BHU inside a larger space where $< \rho_m/2 + \rho_R > \simeq 0$ because the BHU content is negligible when average over a much larger outside volume M_+. This also represents a BH inside our Universe. The second case corresponds to a BHU that is causally disconnected from the rest of space-time. The observational fact that $\rho_\Lambda \sim \rho_m$ seems to agree well with this second solution (Gaztañaga 2021). This agreement (the coincidence problem) seems to be telling us that the light-cone volume outside our BHU is not very large. But note that $< \rho_m/2 + \rho_R > \simeq \Delta$ if matter and radiation are generated by some reheating (see §2.1). DE, inflation and BH interior seem different aspects of the same BHU solution.

[2] See: https://darkcosmos.com/home/f/keplers-laws.